

Closing the equations of motion of anisotropic fluid dynamics by a judicious choice of moment of the Boltzmann equation

E. Molnár,¹ H. Niemi,¹ and D. H. Rischke¹

¹*Institut für Theoretische Physik, Johann Wolfgang Goethe-Universität,
Max-von-Laue-Str. 1, D-60438 Frankfurt am Main, Germany*

In Molnár *et al.* [Phys. Rev. D **93**, 114025 (2016)] the equations of anisotropic dissipative fluid dynamics were obtained from the moments of the Boltzmann equation based on an expansion around an arbitrary anisotropic single-particle distribution function. In this paper we make a particular choice for this distribution function and consider the boost-invariant expansion of a fluid in one dimension. In order to close the conservation equations, we need to choose an additional moment of the Boltzmann equation. We discuss the influence of the choice of this moment on the time evolution of fluid-dynamical variables and identify the moment that provides the best match of anisotropic fluid dynamics to the solution of the Boltzmann equation in the relaxation-time approximation.

PACS numbers: 12.38.Mh, 24.10.Nz, 47.75.+f, 51.10+y

I. INTRODUCTION

Relativistic fluid dynamics has been successfully applied to understand a wide variety of phenomena in the fields of astrophysics, cosmology, cold-atoms, and heavy-ion collisions [1–4]. In particular, relativistic dissipative fluid dynamics has become one of the main tools in understanding the dynamics and properties of strongly interacting matter formed in ultrarelativistic heavy-ion collisions at BNL’s Relativistic Heavy Ion Collider (RHIC) and at CERN’s Large Hadron Collider (LHC). Such investigations have led to tremendous progress in our understanding of the properties of such matter, e.g. its equation of state and transport coefficients [5–10]. A necessary prerequisite for these investigations is, however, to know the regime of applicability and limitations of relativistic fluid dynamics.

The applicability of traditional dissipative fluid-dynamical theories is restricted to the vicinity of local thermodynamical equilibrium. This implies that the deviations of the single-particle distribution function from its form in local thermodynamical equilibrium are small. However, the system formed in relativistic heavy-ion collisions is not macroscopically large and it undergoes rapid expansion. Such conditions are challenging for fluid dynamics, as this can create situations where momentum-space anisotropies are of major significance. In particular, this is true in the very early stages of heavy-ion collisions.

To overcome such limitations of fluid-dynamical theories, in the late 1980’s Barz, Kämpfer, Lukács, Martínás, and Wolf [11] proposed an energy-momentum tensor which incorporated the momentum anisotropy in terms of a space-like four-vector l^μ . Quite recently, two research groups aimed at including a large momentum-space anisotropy into the fluid-dynamical framework for ultrarelativistic heavy-ion collisions. Florkowski and Ryblewski [12–16] and Martinez and Strickland [17–19] effectively rediscovered anisotropic fluid dynamics and initiated a new line of research, cf. Refs. [20–23].

Their approach is based on a single-particle distribution function in momentum space, termed $\hat{f}_{0\mathbf{k}}$ in the following, which is a deformed ellipsoid in the local rest (LR) frame of matter [24]. The momentum-space anisotropy is controlled by a single parameter ξ , such that $\lim_{\xi \rightarrow 0} \hat{f}_{0\mathbf{k}} = f_{0\mathbf{k}}$, where $f_{0\mathbf{k}}$ is the single-particle distribution function in local thermodynamical equilibrium, which is isotropic in the LR frame. In anisotropic fluid dynamics the momentum-space anisotropy can in principle be arbitrarily large, which is in contrast to conventional dissipative fluid dynamics, which is based on the assumption of small deviations from local equilibrium.

The particle number four-current \hat{N}^μ and energy-momentum tensor $\hat{T}^{\mu\nu}$ are given by the first and second moments of $\hat{f}_{0\mathbf{k}}$. The difference compared to an ideal fluid, where $f_{0\mathbf{k}}$ is the single-particle distribution function, is that now the conserved quantities are functions of the parameters ξ and l^μ , in addition to temperature T , chemical potential μ , and fluid four-velocity u^μ , which specify $f_{0\mathbf{k}}$. Therefore, the conservation equations and the equation of state do no longer form a closed set of equations, and additional equations determining ξ and l^μ are needed. Usually, l^μ is fixed by the requirement that it is orthogonal to u^μ , $u_\mu l^\mu = 0$, and normalized, $l_\mu l^\mu = -1$. For the sake of simplicity it may be chosen to have no components in the plane transverse to the beam (z -)direction, such that $l^\mu = \gamma_z (v_z, 0, 0, 1)$, where $\gamma_z = (1 - v_z^2)^{-1/2}$. Thus, only one additional equation is needed, which determines the time evolution of ξ .

If the particle number (or, in the relativistic context, net-charge) is conserved, the zeroth moment of the Boltzmann equation provides the corresponding conservation equation. However, in situations where particle number (or net-charge) is not conserved (for instance, when particles are produced or annihilated), the zeroth moment of the collision term does not vanish. The zeroth moment of the Boltzmann equation can then be used to determine the momentum-space anisotropy. However, due to fact that there is an infinite hierarchy of moment equations,

also higher moments of the Boltzmann equation could be used to provide closure of the equations of motion. This strategy was employed in Refs. [25–28], where specific projections of the second moment of the Boltzmann equation were used.

In principle, the ambiguity in the choice of moment can be resolved by comparing the fluid-dynamical solution to that of the Boltzmann equation. This is the purpose of the present paper. We study several possible choices for the moment that closes the equations of motion, both in the case with and without particle-number conservation.

The paper is organized as follows. In Sec. II we recall the tensor decomposition and the equations of motion in the case of an arbitrary anisotropic distribution function from Ref. [29]. In Sec. III we apply this formalism to a specific example, the so-called Romatschke-Strickland distribution function, and provide the Landau matching conditions to calculate temperature and, in the case of particle-number conservation, chemical potential. Assuming 0+1 dimensional Bjorken flow [30] and the relaxation-time approximation (RTA) for the collision term [31, 32], we present the conservation equations and the various choices for the moment equation which is used to provide closure. In Sec. IV we systematically study these choices and compare them to the solution of the Boltzmann equation. We conclude this work in Sec. V with a summary and an outlook. Technical details are relegated to the Appendices.

We adopt natural units, $\hbar = c = k_B = 1$, throughout this work. The elementary projection operator orthogonal to u^μ is denoted by $\Delta^{\mu\nu} = g^{\mu\nu} - u^\mu u^\nu$, where $g^{\mu\nu} = g_{\nu\mu} = \text{diag}(1, -1, -1, -1)$ is the Minkowski metric tensor of flat space-time. The four-momentum of particles, $k^\mu = (k_0, k_x, k_y, k_z)$ is normalized to the rest mass m_0 of the particles, $k^\mu k_\mu = m_0^2$, and can be decomposed into two parts, $k^\mu = E_{\mathbf{k}u} u^\mu + k^{\{\mu\}}$, where $E_{\mathbf{k}u} = k^\mu u_\mu$ is the (relativistic on-shell) energy, while $k^{\{\mu\}} = \Delta^{\mu\nu} k_\nu$ is the particle momentum orthogonal to the flow velocity. For an arbitrary anisotropy the projection tensor orthogonal to both u^μ and l^μ will be denoted by $\Xi^{\mu\nu} \equiv g^{\mu\nu} - u^\mu u^\nu + l^\mu l^\nu = \Delta^{\mu\nu} + l^\mu l^\nu$ [33–36]. Thus, the four-momentum of particles can be decomposed as $k^\mu = E_{\mathbf{k}u} u^\mu + E_{\mathbf{k}l} l^\mu + k^{\{\mu\}}$, where $E_{\mathbf{k}l} = -k^\mu l_\mu$ is the particle momentum in the direction of the anisotropy and $k^{\{\mu\}} = \Xi^{\mu\nu} k_\nu$ are the components of the momentum orthogonal to both u^μ and l^μ .

II. THE GENERAL EQUATIONS OF MOTION OF ANISOTROPIC FLUIDS

The starting point of relativistic kinetic theory is the Boltzmann equation [37, 38],

$$k^\mu \partial_\mu f_{\mathbf{k}} = C[f], \quad (1)$$

where $f_{\mathbf{k}} = f(x^\mu, k^\mu)$ is the single-particle distribution function at space-time coordinate x^μ , while $\partial_\mu \equiv \partial/\partial x^\mu$

is the space-time derivative. The collision integral (for binary collisions only) is

$$C[f] = \frac{1}{2} \int dK' dP dP' W_{\mathbf{k}\mathbf{k}' \rightarrow \mathbf{p}\mathbf{p}'} \times \left(f_{\mathbf{p}} f_{\mathbf{p}'} \tilde{f}_{\mathbf{k}} \tilde{f}_{\mathbf{k}'} - f_{\mathbf{k}} f_{\mathbf{k}'} \tilde{f}_{\mathbf{p}} \tilde{f}_{\mathbf{p}'} \right). \quad (2)$$

Here, $\tilde{f}_{\mathbf{k}} = 1 - a f_{\mathbf{k}}$, where $a = \pm 1$ for fermions/bosons, while $a = 0$ corresponds to classical, indistinguishable particles. The invariant momentum-space volume is $dK = g d^3 \mathbf{k} / [(2\pi)^3 k^0]$, where g denotes the number of internal degrees of freedom. Furthermore, $W_{\mathbf{k}\mathbf{k}' \rightarrow \mathbf{p}\mathbf{p}'}$ is the invariant transition rate.

Following Ref. [29] we denote the anisotropic distribution function as $\hat{f}_{0\mathbf{k}}(\hat{\alpha}, \hat{\beta}_u E_{\mathbf{k}u}, \hat{\beta}_l E_{\mathbf{k}l})$, which characterizes an anisotropic state as a function of three scalar parameters, $\hat{\alpha}$, $\hat{\beta}_u$, and $\hat{\beta}_l$, as well as the on-shell energy $E_{\mathbf{k}u}$ and the momentum component $E_{\mathbf{k}l}$ in the direction of the anisotropy. We also demand that

$$\lim_{\hat{\beta}_l \rightarrow 0} \hat{f}_{0\mathbf{k}}(\hat{\alpha}, \hat{\beta}_u E_{\mathbf{k}u}, \hat{\beta}_l E_{\mathbf{k}l}) = f_{0\mathbf{k}}(\hat{\alpha}, \hat{\beta}_u E_{\mathbf{k}u}), \quad (3)$$

i.e., in the limit of vanishing anisotropy parameter $\hat{\beta}_l$ the anisotropic distribution converges to the distribution function in local thermodynamical equilibrium. This is the so-called Jüttner distribution function [39, 40],

$$f_{0\mathbf{k}}(\alpha_0, \beta_0 E_{\mathbf{k}u}) = [\exp(-\alpha_0 + \beta_0 E_{\mathbf{k}u}) + a]^{-1}, \quad (4)$$

where $\beta_0 = 1/T$ and $\alpha_0 = \mu/\beta_0$.

The moments of tensor rank n of the anisotropic distribution function $\hat{f}_{0\mathbf{k}}$ are defined as

$$\hat{\mathcal{I}}_{ij}^{\mu_1 \dots \mu_n} = \left\langle E_{\mathbf{k}u}^i E_{\mathbf{k}l}^j k^{\mu_1} \dots k^{\mu_n} \right\rangle_{\hat{0}}, \quad (5)$$

where $\langle \dots \rangle_{\hat{0}} = \int dK (\dots) \hat{f}_{0\mathbf{k}}$. These moments are expanded as

$$\hat{\mathcal{I}}_{ij}^{\mu_1 \dots \mu_n} = \sum_{q=0}^{[n/2]} \sum_{r=0}^{n-2q} (-1)^q b_{nrq} \hat{\mathcal{I}}_{i+j+n, j+r, q} \times \Xi^{(\mu_1 \mu_2 \dots \mu_{2q-1} \mu_{2q})} l^{\mu_{2q+1}} \dots l^{\mu_{2q+r}} u^{\mu_{2q+r+1}} \dots u^{\mu_n}, \quad (6)$$

where n , r , and q are natural numbers and $[n/2]$ denotes the integer part of $n/2$. The number of permutations of indices that lead to distinct tensors $\Xi(\dots l \dots u)$ is $b_{nrq} = n! (2q-1)! / [(2q)! r! (n-2q-r)!]$. The double factorials of even and odd numbers are defined as $(2q)!! = 2^q q!$ and $(2q-1)!! = (2q)! / (2^q q!)$, respectively. Finally, the generalized thermodynamic integrals are defined as

$$\hat{\mathcal{I}}_{nrq} = \frac{(-1)^q}{(2q)!!} \left\langle E_{\mathbf{k}u}^{n-r-2q} E_{\mathbf{k}l}^r (\Xi^{\mu\nu} k_\mu k_\nu)^q \right\rangle_{\hat{0}}. \quad (7)$$

Note that in analogy to Eq. (5) we define the generalized moments of $f_{0\mathbf{k}}$ as

$$\lim_{\hat{\beta}_l \rightarrow 0} \hat{\mathcal{I}}_{ij}^{\mu_1 \dots \mu_n} \equiv \mathcal{I}_{ij}^{\mu_1 \dots \mu_n} = \left\langle E_{\mathbf{k}u}^i E_{\mathbf{k}l}^j k^{\mu_1} \dots k^{\mu_n} \right\rangle_0, \quad (8)$$

where $\langle \dots \rangle_0 = \int dK (\dots) f_{0\mathbf{k}}$. The thermodynamic integrals in equilibrium are thus given by

$$I_{nrq} = \lim_{\hat{\beta}_l \rightarrow 0} \hat{I}_{nrq}, \quad (9)$$

i.e., they are given by Eq. (7) upon replacing $\langle \dots \rangle_{\hat{0}} \rightarrow \langle \dots \rangle_0$.

Using the expansion (6), we readily obtain the conserved quantities $\hat{N}^\mu \equiv \hat{\mathcal{I}}_{00}^\mu$ and $\hat{T}^{\mu\nu} \equiv \hat{\mathcal{I}}_{00}^{\mu\nu}$ decomposed with respect to u^μ , l^ν , and $\Xi^{\mu\nu}$,

$$\hat{N}^\mu \equiv \langle k^\mu \rangle_{\hat{0}} = \hat{n}u^\mu + \hat{n}_l l^\mu, \quad (10)$$

$$\hat{T}^{\mu\nu} \equiv \langle k^\mu k^\nu \rangle_{\hat{0}} = \hat{e}u^\mu u^\nu + 2\hat{M}u^{(\mu} l^{\nu)} + \hat{P}_l l^\mu l^\nu - \hat{P}_\perp \Xi^{\mu\nu}. \quad (11)$$

The coefficients of the various tensor structures can be expressed in terms of generalized thermodynamic integrals or, equivalently, by different projections of the tensor moments (5),

$$\hat{n} \equiv \hat{N}^\mu u_\mu = \hat{I}_{100} = \hat{\mathcal{I}}_{10}, \quad (12)$$

$$\hat{n}_l \equiv -\hat{N}^\mu l_\mu = \hat{I}_{110} = \hat{\mathcal{I}}_{01}, \quad (13)$$

$$\hat{e} \equiv \hat{T}^{\mu\nu} u_\mu u_\nu = \hat{I}_{200} = \hat{\mathcal{I}}_{20}, \quad (14)$$

$$\hat{M} \equiv -\hat{T}^{\mu\nu} u_\mu l_\nu = \hat{I}_{210} = \hat{\mathcal{I}}_{11}, \quad (15)$$

$$\hat{P}_l \equiv \hat{T}^{\mu\nu} l_\mu l_\nu = \hat{I}_{220} = \hat{\mathcal{I}}_{02}, \quad (16)$$

$$\hat{P}_\perp \equiv -\frac{1}{2} \hat{T}^{\mu\nu} \Xi_{\mu\nu} = \hat{I}_{201} = -\frac{1}{2} (m_0^2 \hat{\mathcal{I}}_{00} - \hat{\mathcal{I}}_{20} + \hat{\mathcal{I}}_{02}). \quad (17)$$

The particle density is \hat{n} , and \hat{n}_l is the part of the particle diffusion current that points into the l^μ -direction. The energy density is \hat{e} , while \hat{M} is the part of the energy diffusion current along the l^μ -direction. The pressure component in the direction of the momentum anisotropy is \hat{P}_l , while the pressure in the direction transverse to l^μ is \hat{P}_\perp . The isotropic pressure is defined as

$$\hat{P} \equiv -\frac{1}{3} \hat{T}^{\mu\nu} \Delta_{\mu\nu} = \frac{1}{3} (\hat{P}_l + 2\hat{P}_\perp). \quad (18)$$

Therefore, the particle four-current and energy-momentum tensor defined in Eqs. (10) and (11) contain nine unknowns: the four-vector u^μ with three independent components and six scalars, \hat{n} , \hat{e} , \hat{n}_l , \hat{M} , \hat{P}_l , and \hat{P}_\perp . (We assume that l^μ is already fixed as described in Sec. I.) However, since these latter quantities are functions of three independent scalars $\hat{\alpha}$, $\hat{\beta}_u$, and $\hat{\beta}_l$, only three of the above six scalar variables are independent.

One still needs to assign a physical meaning to the fluid four-velocity, i.e., one needs to determine which physical quantity is actually at rest in the LR frame. Eckart's choice [41] is the flow of particles,

$$u^\mu \equiv \frac{\hat{N}^\mu}{\sqrt{\hat{N}^\nu \hat{N}_\nu}}. \quad (19)$$

This implies that there is no particle diffusion, i.e., $\hat{n}_l = 0$. Landau and Lifshitz [42] choose to define the LR frame in terms of the flow of energy,

$$u^\mu \equiv \frac{\hat{T}^{\mu\nu} u_\nu}{\sqrt{u^\lambda \hat{T}_{\alpha\lambda} \hat{T}^{\alpha\beta} u_\beta}}, \quad (20)$$

which leads to a vanishing energy diffusion current, i.e., $\hat{M} = 0$.

However, neither of these choices removes one of the six unknowns u^μ , $\hat{\alpha}$, $\hat{\beta}_u$, and $\hat{\beta}_l$. The conservation equations, $\partial_\mu \hat{N}^\mu = 0$ and $\partial_\mu \hat{T}^{\mu\nu} = 0$, provide only five constraints for these six independent variables, hence we need an additional equation for the remaining variable. Naturally, in kinetic theory this can be provided by choosing an equation from the infinite hierarchy of moment equations of the Boltzmann equation. For an anisotropic distribution function these equations have the following form

$$\partial_\lambda \hat{\mathcal{I}}_{00}^{\mu_1 \dots \mu_n \lambda} = \hat{\mathcal{C}}_{00}^{\mu_1 \dots \mu_n}, \quad (21)$$

where the collision integral is defined as

$$\hat{\mathcal{C}}_{ij}^{\mu_1 \dots \mu_n} = \int dK E_{\mathbf{k}u}^i E_{\mathbf{k}l}^j k^{\mu_1} \dots k^{\mu_n} C[\hat{f}_{0\mathbf{k}}]. \quad (22)$$

Contracting Eq. (21) with projection tensors built from u^μ , l^ν , and $\Xi^{\mu\nu}$ leads to the following tensor equations,

$$\begin{aligned} & u_{\mu_1} \dots u_{\mu_i} l_{\mu_{i+1}} \dots l_{\mu_{i+j}} \Xi_{\mu_{i+j+1} \dots \mu_n}^{\alpha_i + j + 1 \dots \alpha_n} \partial_\lambda \hat{\mathcal{I}}_{00}^{\mu_1 \dots \mu_n \lambda} \\ &= u_{\mu_1} \dots u_{\mu_i} l_{\mu_{i+1}} \dots l_{\mu_{i+j}} \Xi_{\mu_{i+j+1} \dots \mu_n}^{\alpha_i + j + 1 \dots \alpha_n} \hat{\mathcal{C}}_{00}^{\mu_1 \dots \mu_n}, \end{aligned} \quad (23)$$

where $\Xi_{\nu_1 \dots \nu_n}^{\mu_1 \dots \mu_n}$ are irreducible projection operators constructed from the $\Xi^{\mu\nu}$'s, such that for any $n \geq 2$ they are symmetric, traceless, and orthogonal to both u^μ and l^ν .

In Ref. [29] we derived the equations of motion for the irreducible moments $\hat{\rho}_{ij}^{\mu_1 \dots \mu_\ell}$ of $\delta \hat{f}_{\mathbf{k}} \equiv f_{\mathbf{k}} - \hat{f}_{0\mathbf{k}}$. Although we only wrote them down explicitly up to tensor rank $n = 2$, they follow from a tensor equation similar to Eq. (23). The latter is then simply the special case of that tensor equation obtained by setting $\hat{\rho}_{ij}^{\mu_1 \dots \mu_\ell} \equiv 0$. Ultimately, we can take the equation for the scalar moment, Eq. (110) of Ref. [29], and put all irreducible moments $\hat{\rho}_{ij}^{\mu_1 \dots \mu_\ell} \equiv 0$ to obtain

$$\begin{aligned} \hat{\mathcal{C}}_{i-1,j} &= D \hat{\mathcal{I}}_{ij} - \left(i \hat{\mathcal{I}}_{i-1,j+1} + j \hat{\mathcal{I}}_{i+1,j-1} \right) l_\alpha D u^\alpha \\ &\quad - D_l \hat{\mathcal{I}}_{i-1,j+1} + \left[(i-1) \hat{\mathcal{I}}_{i-2,j+2} + (j+1) \hat{\mathcal{I}}_{ij} \right] l_\alpha D_l u^\alpha \\ &\quad - \frac{1}{2} \left[m_0^2 (i-1) \hat{\mathcal{I}}_{i-2,j} - (i+1) \hat{\mathcal{I}}_{ij} + (i-1) \hat{\mathcal{I}}_{i-2,j+2} \right] \tilde{\theta} \\ &\quad + \frac{1}{2} \left[m_0^2 j \hat{\mathcal{I}}_{i-1,j-1} - j \hat{\mathcal{I}}_{i+1,j-1} + (j+2) \hat{\mathcal{I}}_{i-1,j+1} \right] \tilde{\theta}_l. \end{aligned} \quad (24)$$

Similarly, taking Eq. (111) of Ref. [29] and setting all irreducible moments $\hat{\rho}_{ij}^{\mu_1 \dots \mu_\ell} \equiv 0$ we obtain the equation

for the vector moment,

$$\begin{aligned}
2\hat{\mathcal{C}}_{i-1,j}^{\{\mu\}} &= \tilde{\nabla}^\mu \left(m_0^2 \hat{\mathcal{L}}_{i-1,j} - \hat{\mathcal{L}}_{i+1,j} + \hat{\mathcal{L}}_{i-1,j+2} \right) \\
&- \left[m_0^2 i \hat{\mathcal{L}}_{i-1,j} - (i+2) \hat{\mathcal{L}}_{i+1,j} + i \hat{\mathcal{L}}_{i-1,j+2} \right] \Xi_\alpha^\mu D u^\alpha \\
&+ \left[m_0^2 j \hat{\mathcal{L}}_{i,j-1} - j \hat{\mathcal{L}}_{i+2,j-1} + (j+2) \hat{\mathcal{L}}_{i,j+1} \right] \Xi_\alpha^\mu D l^\alpha \\
&+ \left[m_0^2 (i-1) \hat{\mathcal{L}}_{i-2,j+1} - (i+1) \hat{\mathcal{L}}_{i,j+1} \right] \Xi_\alpha^\mu D l u^\alpha \\
&- \left[m_0^2 (j+1) \hat{\mathcal{L}}_{i-1,j} - (j+1) \hat{\mathcal{L}}_{i+1,j} \right] \Xi_\alpha^\mu D l^\alpha \\
&+ (i-1) \hat{\mathcal{L}}_{i-2,j+3} \Xi_\alpha^\mu D l u^\alpha - (j+3) \hat{\mathcal{L}}_{i-1,j+2} \Xi_\alpha^\mu D l^\alpha \\
&- (i-1) \left(m_0^2 \hat{\mathcal{L}}_{i-2,j+1} - \hat{\mathcal{L}}_{i,j+1} + \hat{\mathcal{L}}_{i-2,j+3} \right) l_\alpha \tilde{\nabla}^\mu u^\alpha \\
&- j \left(m_0^2 \hat{\mathcal{L}}_{i,j-1} - \hat{\mathcal{L}}_{i+2,j-1} + \hat{\mathcal{L}}_{i,j+1} \right) l_\alpha \tilde{\nabla}^\mu u^\alpha . \quad (25)
\end{aligned}$$

Here, $D = u^\mu \partial_\mu$ denotes the comoving derivative and $D_l = -l^\mu \partial_\mu$ is the derivative in the direction of the anisotropy. The spatial gradient in the directions orthogonal to both u^μ and l^μ is $\tilde{\nabla}_\mu = \Xi_{\mu\nu} \partial^\nu$, while the expansion scalars are defined as $\tilde{\theta} = \tilde{\nabla}_\mu u^\mu$ and $\tilde{\theta}_l = \tilde{\nabla}_\mu l^\mu$.

The particle-number conservation equation follows from Eq. (24) by choosing $i = 1$ and $j = 0$. Using Eqs. (12)–(17) we obtain

$$\begin{aligned}
0 = \partial_\mu \hat{N}^\mu &\equiv D \hat{n} - D_l \hat{n}_l + \hat{n} \tilde{\theta} + \hat{n}_l \tilde{\theta}_l \\
&+ \hat{n} l_\mu D_l u^\mu - \hat{n}_l l_\mu D u^\mu , \quad (26)
\end{aligned}$$

where due to particle-number conservation $\hat{\mathcal{C}}_{00} = 0$.

The energy-conservation equation follows from Eq. (24) by choosing $i = 2$ and $j = 0$,

$$\begin{aligned}
0 = u_\nu \partial_\mu \hat{T}^{\mu\nu} &\equiv D \hat{e} - D_l \hat{M} + \left(\hat{e} + \hat{P}_\perp \right) \tilde{\theta} + \hat{M} \tilde{\theta}_l \\
&+ \left(\hat{e} + \hat{P}_l \right) l_\mu D_l u^\mu - 2 \hat{M} l_\mu D u^\mu , \quad (27)
\end{aligned}$$

while the conservation equation for the momentum in the l^μ -direction can be obtained for $i = 1$ and $j = 1$,

$$\begin{aligned}
0 = l_\nu \partial_\mu \hat{T}^{\mu\nu} &\equiv -D \hat{M} + D_l \hat{P}_l - \hat{M} \tilde{\theta} + \left(\hat{P}_\perp - \hat{P}_l \right) \tilde{\theta}_l \\
&- 2 \hat{M} l_\mu D_l u^\mu + \left(\hat{e} + \hat{P}_l \right) l_\mu D u^\mu , \quad (28)
\end{aligned}$$

where $\hat{\mathcal{C}}_{10} = 0$ and $\hat{\mathcal{C}}_{01} = 0$ vanish due to energy and momentum conservation, respectively.

The conservation equation for the momentum transverse to l^μ can be obtained from Eq. (25) for $i = 1$ and $j = 0$. Using $\hat{\mathcal{C}}_{10}^{\{\mu\}} = 0$ we obtain,

$$\begin{aligned}
0 = \Xi_\nu^\alpha \partial_\mu \hat{T}^{\mu\nu} &\equiv \left(\hat{e} + \hat{P}_\perp \right) \left(D u^\alpha + l^\alpha l_\nu D u^\nu \right) \\
&- \tilde{\nabla}^\alpha \hat{P}_\perp + \left(\hat{P}_\perp - \hat{P}_l \right) \left(D_l l^\alpha + u^\alpha l_\nu D_l u^\nu \right) \\
&+ \hat{M} \left(D l^\alpha + u^\alpha l_\nu D u^\nu \right) - \hat{M} \left(D_l u^\alpha + l^\alpha l_\nu D_l u^\nu \right) . \quad (29)
\end{aligned}$$

In order to close the five conservation equations in terms of fluid-dynamical quantities we need to supply

Eqs. (26)–(29) with an additional equation of motion. To this end, it is natural to select the equation of motion for \hat{n}_l or \hat{M} (depending on the choice of the LR frame), or \hat{P}_l . However, as we have already discussed in the Introduction, alternatively we may use any higher moment of the Boltzmann equation to close the conservation equations. The choice of closure is the main question that we will further investigate in the following sections.

III. APPLICATIONS

A. The Romatschke-Strickland distribution function and properties

As a simple, and at the same time relevant, example we take the anisotropic distribution function introduced by Romatschke and Strickland (RS) [24]

$$\hat{f}_{RS} \equiv \left[\exp \left(-\alpha_{RS} + \beta_{RS} \sqrt{k^\mu k^\nu \Omega_{\mu\nu}} \right) + a \right]^{-1} , \quad (30)$$

where

$$\Omega^{\mu\nu} = u^\mu u^\nu + \xi l^\mu l^\nu . \quad (31)$$

Here, ξ denotes the so-called anisotropy parameter. For $\xi < 0$, \hat{f}_{RS} is a prolate spheroid and for $\xi > 0$ it is an oblate spheroid with respect to the z -axis in momentum space and in the LR frame.

Comparing to Eq. (3) we identify $\hat{\alpha} \equiv \alpha_{RS}$, $\hat{\beta}_u \equiv \beta_{RS}$, and $\hat{\beta}_l \equiv \beta_{RS} \sqrt{\xi}$. Furthermore, in order to calculate the fluid-dynamical quantities using the RS distribution function, we shall introduce a new set of thermodynamic integrals, $\hat{I}_{nrq}^{RS}(\alpha_{RS}, \beta_{RS}, \xi)$, which correspond to the replacement $\hat{f}_{0\mathbf{k}} \rightarrow \hat{f}_{RS}$ in Eq. (7),

$$\hat{I}_{nrq}^{RS} = \frac{(-1)^q}{(2q)!!} \int dK E_{\mathbf{k}u}^{n-r-2q} E_{\mathbf{k}l}^r \left(\Xi^{\mu\nu} k_\mu k_\nu \right)^q \hat{f}_{RS} . \quad (32)$$

These integrals are most easily evaluated for a massless Boltzmann gas, i.e., $m_0 = 0$ and $a = 0$. As shown in Ref. [17] assuming $m_0 = 0$ leads to factorization of the ξ -dependent part,

$$\hat{I}_{nrq}^{RS}(\alpha_{RS}, \beta_{RS}, \xi) = I_{nq}(\alpha_{RS}, \beta_{RS}) R_{nrq}(\xi) , \quad (33)$$

where the standard thermodynamic integrals are

$$I_{nq}(\alpha_0, \beta_0) = \frac{(-1)^q}{(2q+1)!!} \left\langle E_{\mathbf{k}u}^{n-2q} \left(\Delta^{\alpha\beta} k_\alpha k_\beta \right)^q \right\rangle_0 . \quad (34)$$

Considering the tensor decomposition of the first and the second moment of the equilibrium distribution function, $N_0^\mu \equiv I_{10} u^\mu = I_{100} u^\mu$ and $T_0^{\mu\nu} \equiv I_{20} u^\mu u^\nu - I_{21} \Delta^{\mu\nu} = I_{200} u^\mu u^\nu + I_{220} l^\mu l^\nu - I_{201} \Xi^{\mu\nu}$, respectively, the particle density is $n_0 \equiv N_0^\mu u_\mu = I_{100} \equiv I_{10}$, the energy density is $e_0 \equiv T_0^{\mu\nu} u_\mu u_\nu = I_{200} \equiv I_{20}$, and the thermodynamic pressure is $P_0 \equiv -\frac{1}{3} T_0^{\mu\nu} \Delta_{\mu\nu}$. The latter is necessarily isotropic, such that $P_{0l} \equiv T_0^{\mu\nu} l_\mu l_\nu = I_{220}$ and

$P_{0\perp} \equiv -\frac{1}{2}T_0^{\mu\nu}\Xi_{\mu\nu} = I_{201}$ are identical, $P_0 = P_{0l} \equiv P_{0\perp}$. Furthermore, in equilibrium $n_{0l} \equiv -N_0^\mu l_\mu = I_{110} = 0$ and $M_0 \equiv T_0^{\mu\nu}u_\mu l_\nu = I_{210} = 0$.

The first and second moments of the RS distribution function are

$$\hat{N}_{RS}^\mu = \hat{n}u^\mu, \quad (35)$$

$$\hat{T}_{RS}^{\mu\nu} = \hat{e}u^\mu u^\nu + \hat{P}_l l^\mu l^\nu - \hat{P}_\perp \Xi^{\mu\nu}, \quad (36)$$

where the quantities defined in Eqs. (12)–(17) can be written with the help of Eq. (33) as

$$\hat{n} \equiv \hat{I}_{100}^{RS} = n_0(\alpha_{RS}, \beta_{RS}) R_{100}(\xi), \quad (37)$$

$$\hat{e} \equiv \hat{I}_{200}^{RS} = e_0(\alpha_{RS}, \beta_{RS}) R_{200}(\xi), \quad (38)$$

$$\hat{P}_l \equiv \hat{I}_{220}^{RS} = e_0(\alpha_{RS}, \beta_{RS}) R_{220}(\xi), \quad (39)$$

$$\hat{P}_\perp \equiv \hat{I}_{201}^{RS} = P_0(\alpha_{RS}, \beta_{RS}) R_{201}(\xi). \quad (40)$$

The isotropic pressure, Eq. (18), leads to the well-known massless ideal gas relation,

$$\begin{aligned} \hat{P}(\alpha_{RS}, \beta_{RS}, \xi) &\equiv P_0(\alpha_{RS}, \beta_{RS}) R_{200}(\xi) \\ &= \frac{\hat{e}(\alpha_{RS}, \beta_{RS}, \xi)}{3}. \end{aligned} \quad (41)$$

This is similar to

$$P_0(\alpha_{RS}, \beta_{RS}) \equiv \frac{n_0(\alpha_{RS}, \beta_{RS})}{\beta_{RS}} = \frac{e_0(\alpha_{RS}, \beta_{RS})}{3}, \quad (42)$$

which is obtained from Eq. (34). All thermodynamic integrals and ratios R_{nrq} are listed in Appendix A. Note that, for the RS distribution function, $\hat{n}_l \equiv \hat{I}_{110}^{RS} = 0$ and $\hat{M} \equiv \hat{I}_{210}^{RS} = 0$. This means that the fluid-dynamical flow velocity does not depend on our choice of LR frame.

Since chemical potential and temperature are quantities defined exclusively in thermodynamical equilibrium, the parameters of the anisotropic distribution function, α_{RS} , β_{RS} , and ξ , have no real physical meaning. However, one can relate them to chemical potential and temperature, or equivalently α_0 and β_0 , of a “fictitious” equilibrium state by imposing the so-called Landau matching conditions $(\hat{N}_{RS}^\mu - N_0^\mu)u_\mu = 0$ and $(\hat{T}_{RS}^{\mu\nu} - T_0^{\mu\nu})u_\mu u_\nu = 0$, or

$$\hat{n}(\alpha_{RS}, \beta_{RS}, \xi) = n_0(\alpha_0, \beta_0), \quad (43)$$

$$\hat{e}(\alpha_{RS}, \beta_{RS}, \xi) = e_0(\alpha_0, \beta_0). \quad (44)$$

Now, using Eqs. (37) and (38) together with Eqs. (A3) and (A10) we obtain

$$\beta_0 = \beta_{RS} \frac{R_{100}(\xi)}{R_{200}(\xi)}, \quad (45)$$

$$\lambda_0 = \lambda_{RS} \frac{[R_{100}(\xi)]^4}{[R_{200}(\xi)]^3}, \quad (46)$$

where $\lambda_0 \equiv \exp \alpha_0 = \exp(\mu\beta_0)$ and $\lambda_{RS} \equiv \exp \alpha_{RS} = \exp(\mu_{RS}\beta_{RS})$ denote the corresponding fugacities. Thus, using Eq. (33) together with these results we obtain the

following general relation between the thermodynamic integrals

$$\hat{I}_{nrq}^{RS}(\alpha_{RS}, \beta_{RS}, \xi) = I_{nq}(\alpha_0, \beta_0) R_{nrq}(\xi) \frac{[R_{200}(\xi)]^{1-n}}{[R_{100}(\xi)]^{2-n}}. \quad (47)$$

However, in case the particle number is not conserved, i.e., $\hat{\alpha} = \alpha_{RS} = 0$, the inverse temperature inferred from the Landau matching condition (44) is

$$\beta_0 = \frac{\beta_{RS}}{[R_{200}(\xi)]^{1/4}}. \quad (48)$$

Thus, similarly to Eq. (47) we now obtain

$$\hat{I}_{nrq}^{RS}(\beta_{RS}, \xi) = I_{nq}(\beta_0) \frac{R_{nrq}(\xi)}{[R_{200}(\xi)]^{(n+2)/4}}. \quad (49)$$

This result was also obtained e.g. in Refs. [13–16] and Refs. [17–19].

After applying the matching conditions we can calculate the equilibrium pressure, $P_0 = P_0(\alpha_0, \beta_0)$, and hence define the bulk viscous pressure

$$\hat{\Pi} \equiv -\frac{1}{3}\hat{T}^{\mu\nu}\Delta_{\mu\nu} = \hat{P}(\alpha_{RS}, \beta_{RS}, \xi) - P_0(\alpha_0, \beta_0), \quad (50)$$

which vanishes for a massless ideal gas, $\lim_{m_0 \rightarrow 0} \hat{\Pi} = 0$.

B. 0+1 dimensional boost-invariant expansion

We now investigate how the solution of the fluid-dynamical equations of motion is influenced by the choice of moment to close them. We study this for a very simple case only, the 0+1 dimensional boost-invariant expansion of matter, known as Bjorken flow [30]. To this end, it is advantageous to transform the usual space-time coordinates (t, z) to proper time $\tau = \sqrt{t^2 - z^2}$ and space-time rapidity $\eta_s = \frac{1}{2} \ln \frac{t+z}{t-z}$. The inverse transformation then reads $t = \tau \cosh \eta_s$ and $z = \tau \sinh \eta_s$. In Bjorken flow, the velocity of matter is given by $v_z \equiv z/t = \tanh \eta_s$, such that

$$u^\mu \equiv \left(\frac{t}{\tau}, 0, 0, \frac{z}{\tau} \right) = (\cosh \eta_s, 0, 0, \sinh \eta_s), \quad (51)$$

$$l^\mu \equiv \left(\frac{z}{\tau}, 0, 0, \frac{t}{\tau} \right) = (\sinh \eta_s, 0, 0, \cosh \eta_s). \quad (52)$$

Then, $D \equiv u^\mu \partial_\mu = \frac{\partial}{\partial \tau}$, $D_l \equiv -l^\mu \partial_\mu = -\frac{\partial}{\partial \eta_s}$, and $Du^\mu = D_l l^\mu = 0$, $D_l u^\mu = -\frac{1}{\tau} l^\mu$, $D_l l^\mu = -\frac{1}{\tau} u^\mu$, while $\tilde{\theta} = \tilde{\theta}_l = 0$. Inserting Eq. (6) into Eq. (24), and using the fact that in Bjorken flow all thermodynamic quantities are independent of η_s , we obtain

$$\frac{\partial \hat{I}_{i+j,j,0}}{\partial \tau} + \frac{1}{\tau} \left[(j+1) \hat{I}_{i+j,j,0} + (i-1) \hat{I}_{i+j,j+2,0} \right] = \hat{C}_{i-1,j}. \quad (53)$$

We also assume that the collision term is given by the relaxation-time approximation (RTA) [31], i.e., $C[\hat{f}] = -\frac{E_{\mathbf{k}u}}{\tau_{eq}} \left(\hat{f}_{0\mathbf{k}} - f_{0\mathbf{k}} \right)$. This means that the anisotropic distribution function $\hat{f}_{0\mathbf{k}}$ is assumed to approach the equilibrium distribution $f_{0\mathbf{k}}$ on a timescale set by τ_{eq} . Thus, in RTA the r.h.s. of Eq. (53) reads

$$\hat{C}_{i-1,j} = -\frac{1}{\tau_{eq}} \left(\hat{I}_{i+j,j,0} - I_{i+j,j,0} \right). \quad (54)$$

For τ_{eq} we will either use a constant value or parametrize it using the relation between τ_{eq} and shear viscosity [43, 44]

$$\tau_{eq}(\tau) = 5\beta_0(\tau) \frac{\eta}{s}, \quad (55)$$

where η/s denotes the ratio of shear viscosity to entropy density, which we assume to take a constant value.

In order to obtain the fluid-dynamical equations of motion for the RS distribution function we substitute $\hat{I}_{nrq} \rightarrow \hat{I}_{nrq}^{RS}$ in Eqs. (53) and (54). Furthermore, using the matching conditions Eqs. (43) and (44), the conservation equations for particle number (26) and energy (27) read

$$\frac{\partial n_0(\alpha_0, \beta_0)}{\partial \tau} + \frac{1}{\tau} n_0(\alpha_0, \beta_0) = 0, \quad (56)$$

and

$$\frac{\partial e_0(\alpha_0, \beta_0)}{\partial \tau} + \frac{1}{\tau} \left[e_0(\alpha_0, \beta_0) + \hat{P}_l(\alpha_{RS}, \beta_{RS}, \xi) \right] = 0. \quad (57)$$

The conservation of momentum in the direction of the anisotropy, Eq. (28), leads to $D\hat{M} = -\hat{M}/\tau$, but since $\hat{M} = 0$ for the RS distribution function, this equation does not provide any additional information. Likewise, the conservation of momentum in the direction transverse to the anisotropy, Eq. (29), gives $\tilde{\nabla}^\alpha \hat{P}_\perp = 0$, which also contains no additional information since the system is homogeneous in the transverse direction.

Now we discuss various choices to close the conservation equations (56) and (57). As mentioned above, in principle there are infinitely many equations that can be selected from the hierarchy of balance equations (21) to serve this purpose. Here we restrict ourselves to a few representative examples. These follow from Eqs. (53) and (54) by choosing particular values for the indices i and j .

(i) $i = 0, j = 2$: This choice gives the time-evolution equation for the longitudinal pressure $\hat{P}_l(\alpha_{RS}, \beta_{RS}, \xi)$,

$$\frac{\partial \hat{P}_l}{\partial \tau} + \frac{1}{\tau} \left(3\hat{P}_l - \hat{I}_{240}^{RS} \right) = -\frac{1}{\tau_{eq}} \left(\hat{P}_l - P_0 \right). \quad (58)$$

Here we can explicitly express \hat{P}_l and \hat{I}_{240}^{RS} via Eq. (47),

$$\hat{P}_l(\alpha_{RS}, \beta_{RS}, \xi) = e_0(\alpha_0, \beta_0) \frac{R_{220}(\xi)}{R_{200}(\xi)}, \quad (59)$$

$$\hat{I}_{240}^{RS}(\alpha_{RS}, \beta_{RS}, \xi) = e_0(\alpha_0, \beta_0) \frac{R_{240}(\xi)}{R_{200}(\xi)}, \quad (60)$$

where the R_{nrq} are listed in Eqs. (A13), (A15), and (A17). Note that Eqs. (59) and (60) are formally unchanged when expressing \hat{P}_l and \hat{I}_{240}^{RS} through Eq. (49). This means that the dynamical equation for \hat{P}_l is a very special choice for closure of the conservation equations, since Eq. (58) is formally independent of whether we conserve particle number or not. Furthermore, as it should be, in the limit of small deviations from local thermodynamical equilibrium, i.e., $\xi \ll 1$, Eqs. (57) and (58) lead precisely to the equations of motion of second-order fluid dynamics as obtained in Refs. [45–48], for more details see App. B.

(ii) $i = 1, j = 0$: This choice was made e.g. in Refs. [17–19]. It is possible only if particle number is not conserved (such that the chemical potential is always zero),

$$\frac{\partial \hat{n}}{\partial \tau} + \frac{1}{\tau} \hat{n} = -\frac{1}{\tau_{eq}} (\hat{n} - n_0). \quad (61)$$

(iii) $i = 3, j = 0$: This choice is analogous to the one of Israel and Stewart [51], which use the second moment of the Boltzmann equation to close the conservation equations,

$$\frac{\partial \hat{I}_{300}^{RS}}{\partial \tau} + \frac{1}{\tau} \left(\hat{I}_{300}^{RS} + 2\hat{I}_{320}^{RS} \right) = -\frac{1}{\tau_{eq}} \left(\hat{I}_{300}^{RS} - I_{300} \right). \quad (62)$$

(iv) $i = 1, j = 2$: This choice is analogous to the previous one, in the sense that it also results from the second moment of the Boltzmann equation,

$$\frac{\partial \hat{I}_{320}^{RS}}{\partial \tau} + \frac{3}{\tau} \hat{I}_{320}^{RS} = -\frac{1}{\tau_{eq}} \left(\hat{I}_{320}^{RS} - I_{320} \right). \quad (63)$$

Note that according to Eq. (23) the cases (iii) and (iv) follow from different projections of $\partial_\lambda \hat{T}^{\mu\nu\lambda} = \hat{C}_{00}^{\mu\nu}$. Also note that the choice $i = 2, j = 1$ is trivial since $\hat{I}_{310}^{RS} = 0$.

Finally, we also tested the following choices:

(v) $i = 0, j = 0$:

$$\frac{\partial \hat{I}_{000}^{RS}}{\partial \tau} + \frac{1}{\tau} \left(\hat{I}_{000}^{RS} - \hat{I}_{020}^{RS} \right) = -\frac{1}{\tau_{eq}} \left(\hat{I}_{000}^{RS} - I_{000} \right). \quad (64)$$

(vi) $i = 0, j = 4$:

$$\frac{\partial \hat{I}_{440}^{RS}}{\partial \tau} + \frac{1}{\tau} \left(5\hat{I}_{440}^{RS} - \hat{I}_{460}^{RS} \right) = -\frac{1}{\tau_{eq}} \left(\hat{I}_{440}^{RS} - I_{440} \right), \quad (65)$$

(vii) $i = 1, j = 4$:

$$\frac{\partial \hat{I}_{540}^{RS}}{\partial \tau} + \frac{5}{\tau} \hat{I}_{540}^{RS} = -\frac{1}{\tau_{eq}} \left(\hat{I}_{540}^{RS} - I_{540} \right). \quad (66)$$

IV. RESULTS AND DISCUSSIONS

In this section, we solve the conservation equations (56) and (57) and study the impact of different ways to

close them, i.e., choosing one of the moment equations (58), (61), (62), (63), (64), (65), or (66). We will also compare the fluid-dynamical solutions to the solution of the Boltzmann equation, in order to identify which one of the moment equations gives the best agreement with the latter.

We always initialize the system with temperature $T_0 = 300$ MeV at initial time $\tau_0 = 1.0$ fm, for three choices of the initial anisotropy, $\xi(\tau_0) \equiv \xi_0 = \{0, 10, 100\}$. We investigate separately the cases with and without particle-number conservation. In the case with particle-number conservation, we take an initial fugacity $\lambda_0 = 1$. The initial value of the temperature and the anisotropy parameter are shown in the headlines of the following figures. If the particle number is conserved, the initial fugacity is also shown. We use either a constant relaxation time $\tau_{eq} = 1$ fm, or the temperature-dependent one from Eq. (55) with $\eta/s = \{1/4\pi, 10/4\pi, 100/4\pi\}$.

For the comparison of the choice of moment in Sec. IV A, we also solve the conservation equations for an ideal fluid, $\frac{\partial e_0}{\partial \tau} + \frac{1}{\tau}(e_0 + P_0) = 0$, where $P_0 \equiv n_0 T_0 = e_0/3$, together with $\frac{\partial n_0}{\partial \tau} + \frac{1}{\tau}n_0 = 0$. Note that in this case the two conservation equations are independent from each other, hence if the system was initially in chemical equilibrium it will stay in chemical equilibrium. Furthermore, in the case of an ideal fluid $\xi(\tau) = 0$, the time evolution of the fugacity is simply given by $\lambda(\tau) = 1$, while the pressure is necessarily isotropic, hence $\hat{P}_l(\tau)/\hat{P}_\perp(\tau) = 1$. These constant horizontal lines are redundant and will not be shown in the respective figures.

A. The choice of moment

The results shown in Fig. 1 were obtained by solving both the particle-number conservation equation (56) and the energy-conservation equation (57), closed by one of the moment equations (58), (62), (63), (64), (65), or (66). Correspondingly, the results in Fig. 2 were obtained without particle-number conservation, i.e., we only solved the energy-conservation equation (57) coupled to a particular moment equation. In this case, the first moment of the Boltzmann equation, Eq. (61), can also be used to provide closure (in addition to the previously listed relaxation equations).

Figure 1 shows the evolution of the anisotropy parameter ξ , temperature T , fugacity λ , and the ratio of longitudinal and transverse pressure components \hat{P}_l/\hat{P}_\perp , as a function of proper time τ . All figures in the left column are for $\xi_0 = 0$, while those in the right column are for $\xi_0 = 10$. In Fig. 2, the same is presented for the case without particle-number conservation.

Focusing on the evolution of the anisotropy parameter ξ we observe that in case the system was initially isotropic ($\xi_0 = 0$, left column), the longitudinal expansion drives the system out of equilibrium. This lasts for about 1–2 fm, after which the system starts to approach the isotropic state again, $\xi \rightarrow 0$. The approach to equilib-

rium becomes much faster for a nonzero initial anisotropy ($\xi_0 = 10$, right column). The late-time behavior is quite similar in both cases, as both reach a similar value for the anisotropy around $\tau \sim 6 - 7$ fm. The behaviour of the longitudinal to transverse pressure ratio, \hat{P}_l/\hat{P}_\perp , is quite similar to that of the anisotropy isotropy parameter. Both the evolution of ξ and \hat{P}_l/\hat{P}_\perp are similar in the cases with and without particle-number conservation, cf. top and bottom rows of Figs. 1 and 2. This can be explained by the fact that \hat{P}_l/\hat{P}_\perp is mainly determined by the momentum anisotropy ξ .

The temperature, second row of Figs. 1 and 2, decreases as the system expands, but the decrease is slower for a nonzero initial anisotropy. This is due to the fact \hat{P}_l decreases with increasing anisotropy, hence the driving force to expand (and cool) the system is smaller for a larger initial anisotropy. Note that for the case without particle-number conservation, Fig. 2, the evolution of the temperature is much closer to the one for an ideal fluid than for the case with particle-number conservation. This holds for all choices of closure of the conservation equations. Vice versa, the spread in the curves is much larger for the case with particle-number conservation, cf. Fig. 1. The reason is that the deviation from chemical equilibrium parametrized by the fugacity, third row of Fig. 1, has to be compensated by an increase in temperature. Thus, the smaller the $\lambda(\tau)$, the larger $T(\tau)$ has to be. This also explains why all curves lie above the case for an ideal fluid (green lines).

These observations are generally valid for all choices of closure for the conservation equations. However, there are striking differences between the various choices. The first observation is that there is a grouping according to the power j of longitudinal momentum E_{kl} appearing in the particular moment $\hat{I}_{i+j,j,0}^{RS}$, cf. \hat{I}_{000}^{RS} and \hat{I}_{300}^{RS} (blue lines), $\hat{P}_l \equiv \hat{I}_{220}^{RS}$ and \hat{I}_{320}^{RS} (black lines), as well as \hat{I}_{440}^{RS} and \hat{I}_{540}^{RS} (red lines). Apparently, the larger the j , the faster the approach to isotropization. This behavior is universal and can be observed in both Figs. 1 and 2.

We also remark that the solutions provided by \hat{I}_{440}^{RS} and \hat{I}_{540}^{RS} stay closer to the solution provided by \hat{P}_l than the ones provided by \hat{I}_{000}^{RS} , \hat{I}_{300}^{RS} , and, in the case without particle-number conservation, \hat{n} . In particular for ξ and \hat{P}_l/\hat{P}_\perp , the latter ones sometimes deviate by more than a factor of two from the solution provided by \hat{P}_l . As we shall see in the next subsection, it turns out that the solution provided by \hat{P}_l is closest to the one of the Boltzmann equation. Note that, in order to improve the agreement of the fluid-dynamical solution given by \hat{n} with the solution of the Boltzmann equation, in some earlier works [43, 44] a rescaled relaxation time $\tau_{eq}^{AH} = \tau_{eq}/2$ was used. We checked that also Eqs. (64) and (62) with τ_{eq}^{AH} instead of τ_{eq} lead to results that resemble the ones for \hat{P}_l . We remark, however, that one is actually not free to adjust the relaxation time in the various moment equations, since in the RTA, cf. Eq. (54), it is the same as the one appearing in the Boltzmann equation.

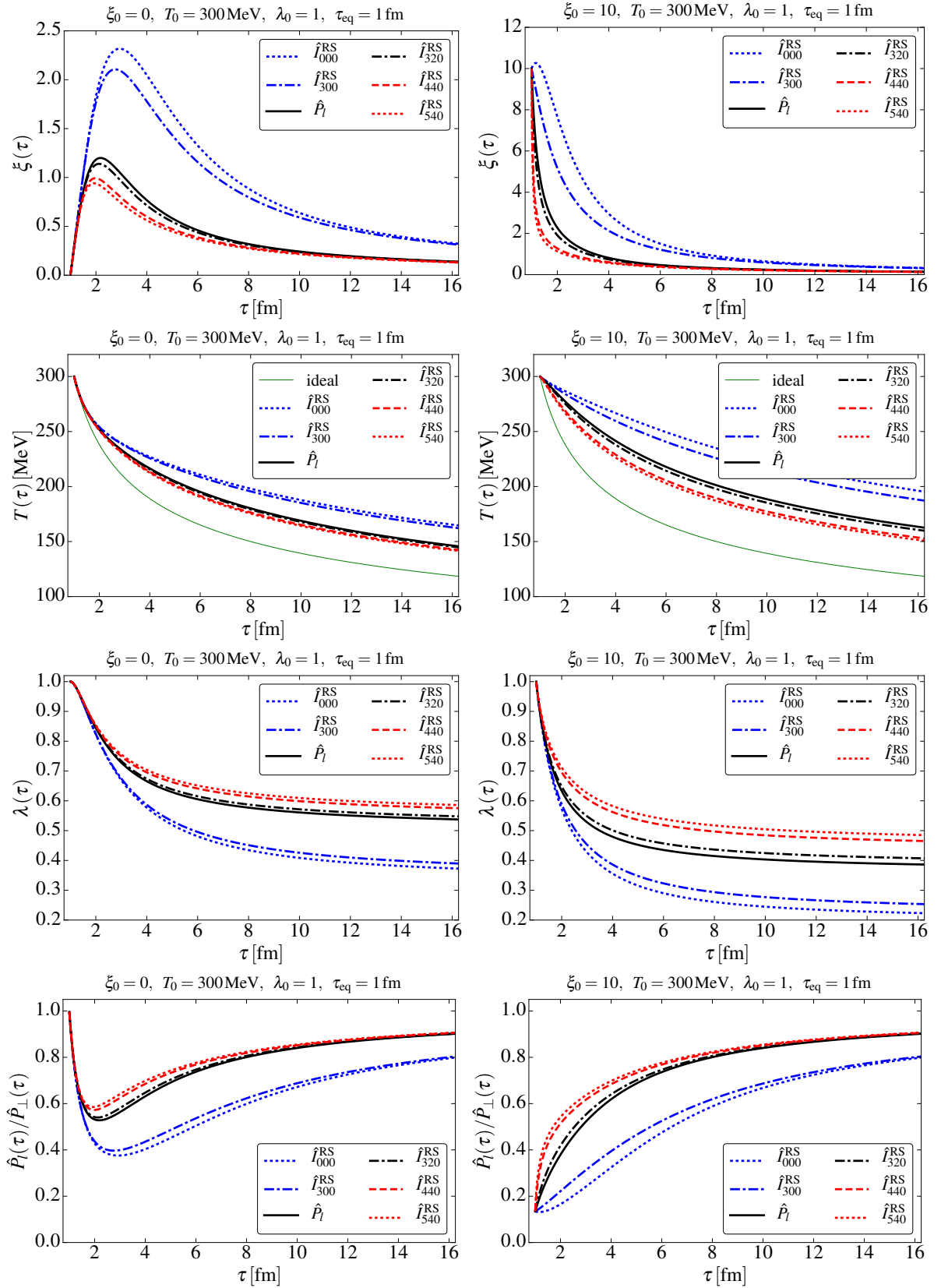


FIG. 1. (Color online) From top to bottom: the evolution of the anisotropy parameter ξ , temperature T , fugacity λ , and the ratio of longitudinal and transverse pressure components \hat{P}_l/\hat{P}_\perp as a function of proper time τ . The thin green line in the figures in the second row represents the temperature evolution for an ideal fluid. The other lines are the solution of the conservation equations (56), (57) closed by different moment equations: the dotted blue line ($\hat{I}_{000}^{\text{RS}}$) corresponds to Eq. (64), the dash-dotted blue line ($\hat{I}_{300}^{\text{RS}}$) to Eq. (62), the full black line (\hat{P}_l) to Eq. (58), the dash-dotted black line ($\hat{I}_{320}^{\text{RS}}$) to Eq. (63), the dashed red ($\hat{I}_{440}^{\text{RS}}$) to Eq. (65), and the dotted red line ($\hat{I}_{540}^{\text{RS}}$) to Eq. (66), respectively.

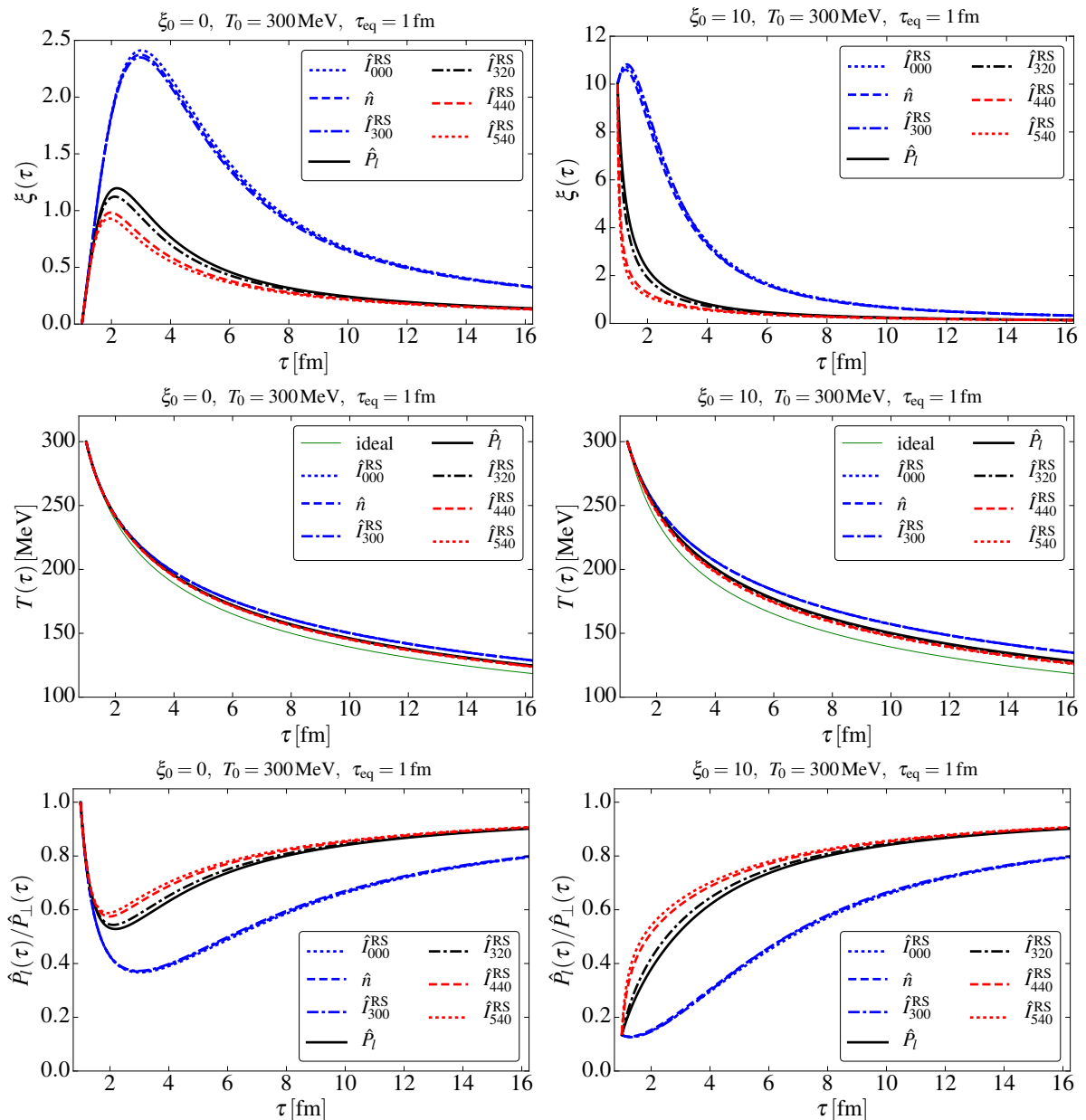


FIG. 2. (Color online) Similar to Fig. 1, but for the case without particle-number conservation, such that always $\lambda(\tau) = 1$ (and thus not explicitly shown). The only difference to Fig. 1 is that now Eq. (61) is available to close the energy-conservation equation. The respective dashed blue line is labelled \hat{n} .

B. Comparisons to the exact solution

In this section we compare the solution of the conservation equations closed by Eq. (58) for \hat{P}_l to the solution of the Boltzmann equation in the RTA. The numerical method to solve the Boltzmann equation is discussed in detail in Refs. [43, 44] as well as in App. C. In analogy to Eq. (7) we introduce the moments of the solution $\hat{f}_{\mathbf{k}}$ of the Boltzmann equation,

$$F_{nrq} = \frac{(-1)^q}{(2q)!!} \int dK E_{\mathbf{k}u}^{n-r-2q} E_{\mathbf{k}l}^r (\Xi^{\mu\nu} k_\mu k_\nu)^q f_{\mathbf{k}}. \quad (67)$$

On the other hand, the moments \hat{I}_{nrq}^{RS} , cf. Eq. (32), can be computed from solving the fluid-dynamical equations, which provide α_0 , β_0 , and ξ required to compute these moments according to Eqs. (47) or (49). We then compare F_{nrq} to \hat{I}_{nrq}^{RS} in order to estimate how much the anisotropic distribution function \hat{f}_{RS} deviates from the full solution of the Boltzmann equation.

In order to compare with the results of Refs. [43, 44] we have also used the temperature-dependent relaxation time from Eq. (55). The solution of the Boltzmann equation is obtained choosing the RS distribution function as the initial condition at proper time $\tau_0 = 1.0$ fm, i.e.,

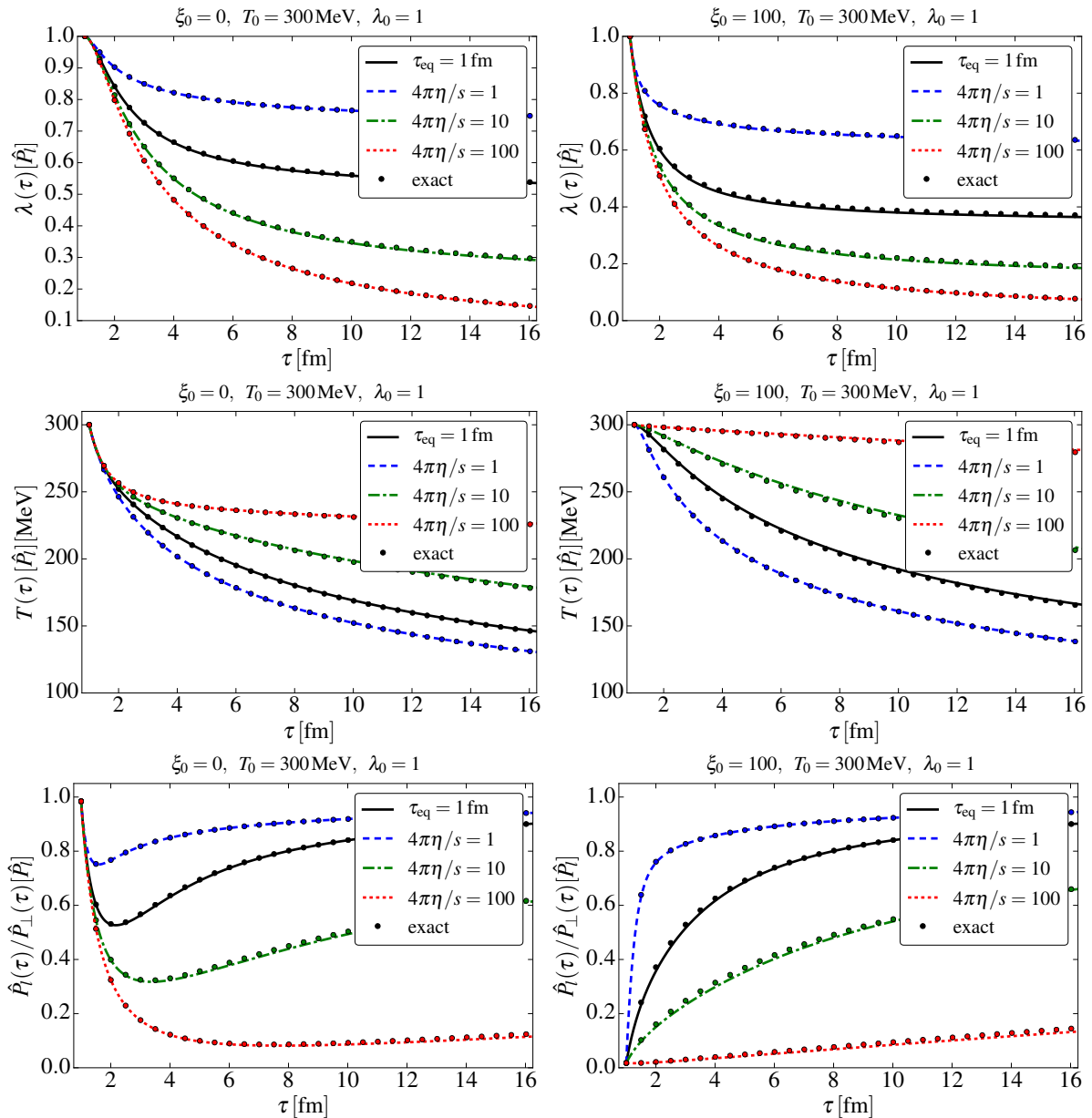


FIG. 3. (Color online) The evolution of temperature T , fugacity λ , and the ratio of longitudinal and transverse pressure components \hat{P}_l/\hat{P}_\perp as a function of proper time τ . The full black, the dashed blue, the dashed-dotted green and the dotted red lines are the solution of the conservation equations closed by the relaxation equation for \hat{P}_l for $\tau_{eq} = 1 \text{ fm}$ and for τ_{eq} from Eq. (55) with the three different choices for η/s . The large dots show the corresponding solution of the Boltzmann equation.

$$f_{\mathbf{k}}(\tau_0) = f_{RS}(\tau_0).$$

In Figs. 3 and 4 the fluid-dynamical solution for a constant relaxation time is shown by the black lines. For $\xi_0 = 0$ (left columns of these figures) these are identical to the black lines in the left columns of Figs. 1 and 2. The other curves in Figs. 3 and 4 correspond to relaxation times chosen according to Eq. (55).

For all quantities shown, the fluid-dynamical solution agrees very well with the exact solution, even for very large $\eta/s = 100/4\pi$, and very large initial anisotropy $\xi_0 = 100$. This is a strong indication that the con-

servation equations closed by the relaxation equation for \hat{P}_l provides the best match to the Boltzmann equation, at least for quantities which appear in the energy-momentum tensor.

Now that we have identified the apparent best match for closure we will investigate how well the other moments of the Boltzmann equation are reproduced using this particular choice for closure. This comparison is shown in Figs. 5 and 6. As can be seen, the very good agreement is not necessarily inherited by other moments. In Fig. 5 we show the ratio of the exact moment F_{320} to

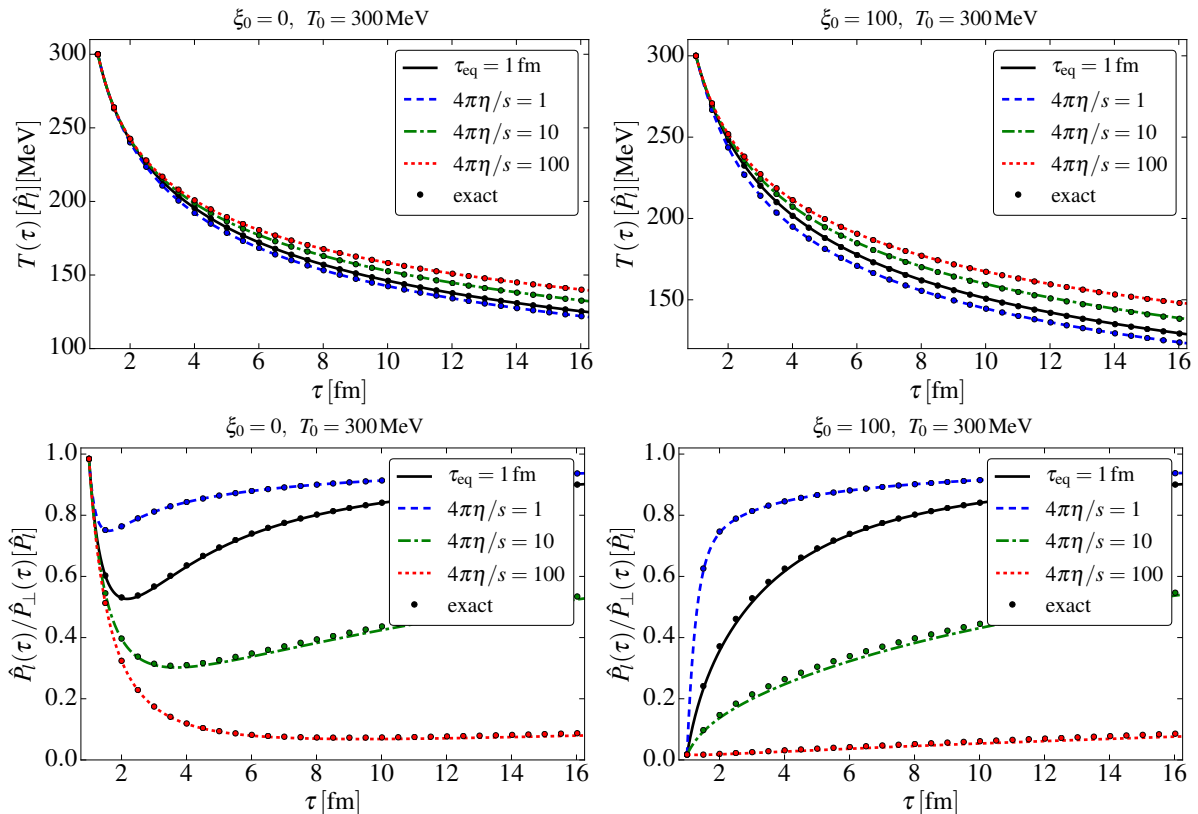


FIG. 4. (Color online) Similar to Fig. 3, but for the case without particle-number conservation (such that $\lambda(\tau) = 1$ and thus not shown explicitly).

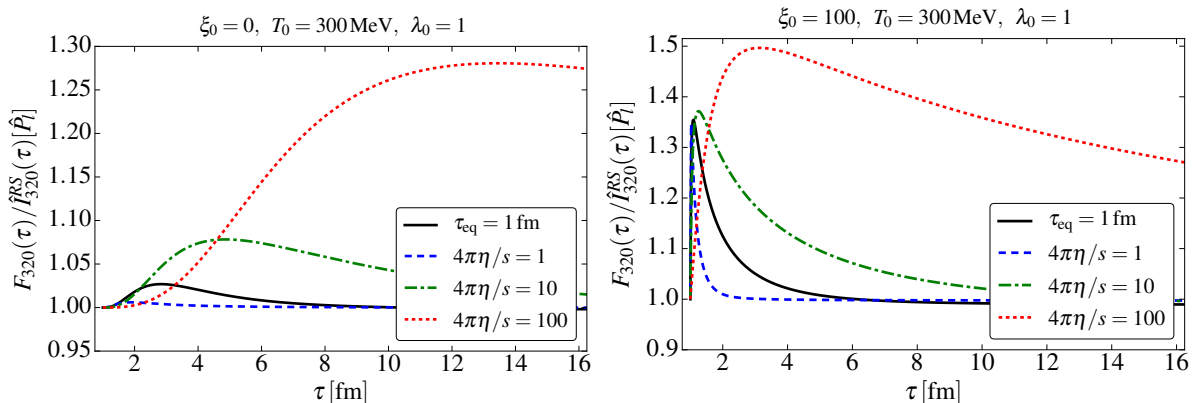


FIG. 5. (Color online) The ratio of the exact solution $F_{320}(\tau)$ to the corresponding fluid-dynamical solution $\hat{F}_{320}^{RS}(\tau)$, obtained from Eqs. (56), (57), and (58). The choice of moment to close the equations is indicated in brackets, $[\hat{P}_\parallel]$, behind the label on the ordinate. The various lines are similar to Figs. 3 and 4.

the fluid-dynamical solution \hat{F}_{320}^{RS} in the case of conserved particle number, and in Fig. 6 the ratio of the exact number density $n \equiv F_{100}$ to $\hat{n} \equiv \hat{F}_{100}^{RS}$ in the case without particle-number conservation. As can be seen, the deviations between the fluid-dynamical and exact solutions can be as large as 50 %, even if the agreement between the primary fluid-dynamical quantities, i.e., the quantities that appear in the energy-momentum tensor itself, is almost perfect. cf. Figs. 3 and 4.

C. Matching to the solution of the Boltzmann equation

In general, a given functional form of the anisotropic distribution function, e.g. \hat{f}_{RS} , does not agree exactly with the solution $f_{\mathbf{k}}$ of the Boltzmann equation. Thus, there is also no reason to expect that all moments \hat{I}_{nrq}^{RS} of \hat{f}_{RS} agree with all moments F_{nrq} of $f_{\mathbf{k}}$. In other words, computing the parameters α_0 , β_0 , and ξ that determine

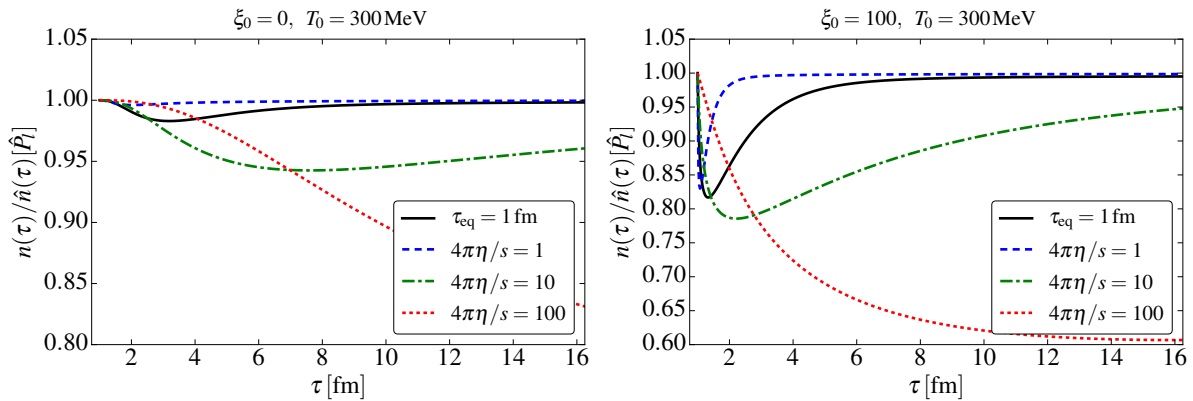


FIG. 6. (Color online) Similar to Fig. 5, but without particle-number conservation. Here $n(\tau) \equiv F_{100}(\tau)$ represents the solution of the Boltzmann equation while $\hat{n}(\tau) \equiv \hat{I}_{100}^{RS}(\tau)$ is computed from the solution of Eqs. (57) and (58). The choice of moment to close the equations is indicated in brackets, $[\hat{P}_i]$, behind the label on the ordinate.

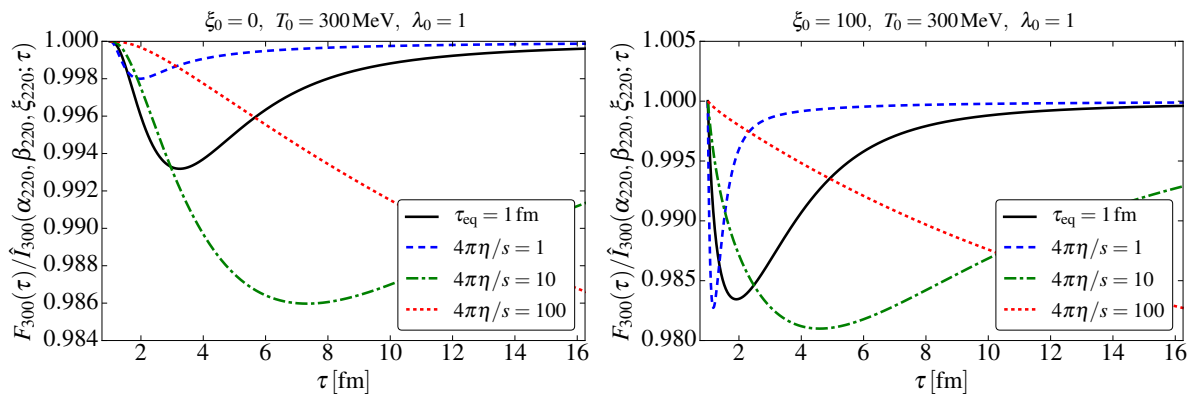


FIG. 7. (Color online) The ratio of the exact solution $F_{300}(\tau)$ to $\hat{I}_{300}^{RS}(\alpha_{220}, \beta_{220}, \xi_{220}; \tau)$, where α_{220} , β_{220} , and ξ_{220} were obtained by matching to $F_{220}(\tau)$. See text for more details.

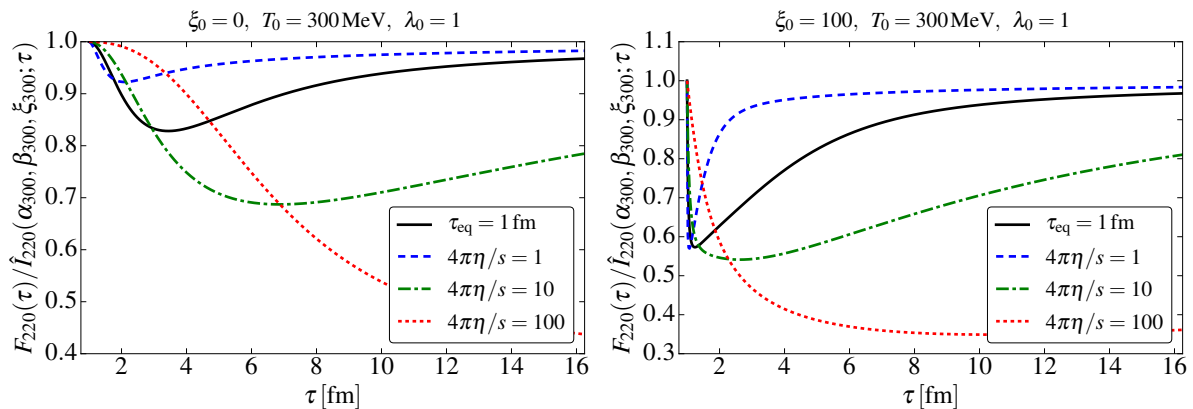


FIG. 8. (Color online) Similar to Fig. 7. The ratio of the exact solution $F_{220}(\tau)$ to $\hat{I}_{220}^{RS}(\alpha_{300}, \beta_{300}, \xi_{300}; \tau)$, where α_{300} , β_{300} , and ξ_{300} were obtained by matching to $F_{300}(\tau)$. See text for more details.

\hat{f}_{RS} from matching a certain *subset* of the moments \hat{I}_{nrq}^{RS} to the moments F_{nrq} of the exact solution, does not necessarily lead to a good agreement for *all* other moments. In this subsection, we provide evidence for this observation through an explicit calculation.

First, however, let us make a few remarks (for the

sake of simplicity we discuss only the case with particle-number conservation):

- The anisotropic distribution function is characterized by three parameters, α_0 , β_0 , and ξ . Correspondingly, three matching conditions are required to determine these parameters.

- The matching conditions can in general be chosen from Eq. (47), for any values of n , r , and q .
- In the RTA the usual Landau matching conditions (43) and (44) are not only convenient, but also necessary to ensure the conservation of energy, momentum, and particle number. These correspond to matching with $(n, r, q) = (2, 0, 0)$ and $(n, r, q) = (1, 0, 0)$. The third matching condition can be provided by any other choice for (n, r, q) .
- When we choose a particular moment equation to close the conservation equations, at the same time we also choose a specific matching condition. For example, closing the system by using Eq. (58) also implies that α_0 , β_0 , and ξ are matched to $\hat{P}_l \equiv \hat{I}_{220}^{RS}$. Alternatively, choosing Eq. (62) implies that they are matched to \hat{I}_{300}^{RS} . Note that in general different choices lead to different values of α_0 , β_0 , and ξ .
- Once the matching conditions are fixed, any other moment can be calculated according to the r.h.s. of Eq. (47).

To further investigate the importance of the matching conditions, we match $\alpha_0(\tau)$, $\beta_0(\tau)$, and $\xi(\tau)$ to a particular moment of the solution of the Boltzmann equation, instead of its fluid-dynamical approximation (53).

In Fig. 7 we use $P_l \equiv F_{220} = \hat{I}_{220}^{RS}(\alpha_{220}, \beta_{220}, \xi_{220}) \equiv \hat{P}_l$ as a matching condition, and plot the ratio of the exact solution F_{300} to the moment $\hat{I}_{300}^{RS}(\alpha_{220}, \beta_{220}, \xi_{220})$ obtained through such a choice of matching [the r.h.s. of Eq. (47)].

In Fig. 8 we show the opposite scenario, i.e., the ratio of F_{220} to $\hat{I}_{220}^{RS}(\alpha_{300}, \beta_{300}, \xi_{300})$ obtained by matching α_{300} , β_{300} , and ξ_{300} to always reproduce the exact moment F_{300} . As can be seen from the figures, if we choose the \hat{P}_l matching, then $\hat{I}_{300}^{RS}(\alpha_{220}, \beta_{220}, \xi_{220})$ is a good approximation to F_{300} , but the opposite is not true: matching to F_{300} does not give the correct $P_l = F_{220} \neq \hat{P}_l(\alpha_{300}, \beta_{300}, \xi_{300})$.

We note that when we solve anisotropic fluid dynamics by choosing Eq. (62), we implicitly use the latter matching. In other words, the values for α_0 , β_0 , and ξ are obtained by matching to \hat{I}_{300}^{RS} , e_0 , and n_0 . However, as can be seen from Fig. 8, the values for \hat{P}_l obtained in this way can deviate by more than 50 % from the exact solution. Since \hat{P}_l appears explicitly in the energy-conservation equation, this deviation in \hat{P}_l will also lead to deviations from the exact solution.

On the other hand, closing the conservation equations with Eq. (58), which corresponds to matching with \hat{P}_l , gives an overall good agreement with the exact solution. The comparison of Figs. 7 and 8 indicates why this is the case: the matching to \hat{P}_l directly leads to the correct driving force in the energy-conservation equation. It is then obvious that this choice gives the best agreement with the Boltzmann equation, as well as smaller deviations from the exact solution for all other moments.

We note that in for the (0+1)-dimensional expansion this choice corresponds to the one proposed in Ref. [49], where the anisotropy parameters were matched to the components of $T^{\mu\nu}$, and the equations of motion were closed by using the exact equations of motion for the dissipative quantities, e.g. for the shear-stress tensor $\pi^{\mu\nu}$. This approach was originally proposed in Ref. [50] for conventional fluid dynamics.

V. CONCLUSIONS

Starting from the relativistic Boltzmann equation, we have derived the equations of motion for a fluid which has a certain anisotropic single-particle distribution function $\hat{f}_{0\mathbf{k}}$ in momentum space in the LR frame. Choosing as an example $\hat{f}_{0\mathbf{k}} = \hat{f}_{RS}$ we have solved these equations in a simple 0+1 dimensional boost-invariant expansion scenario. We have pointed out the importance of the choice of moment equation to close the conservation equations. The solution of the Boltzmann equation was most accurately reproduced by the equations of anisotropic fluid dynamics when the latter are closed using the relaxation equation for the longitudinal pressure P_l , i.e., a quantity which also appears in the energy-momentum tensor. Other choices for the moments to close the conservation equations lead to a less good agreement with the solution of the Boltzmann equation. In the future, one should extend the present study to more realistic geometries (with non-trivial transverse and longitudinal dynamics) and include corrections to $\hat{f}_{0\mathbf{k}}$, using the framework developed in Ref. [29].

ACKNOWLEDGMENTS

The authors thank W. Florkowski, U. Heinz, P. Huovinen, and M. Strickland for comments and suggestions, and M. Strickland for sharing the source code of the Boltzmann equation solver in the RTA. The work of E.M. was partially supported by the Alumni Program of the Alexander von Humboldt Foundation and by BMBF grant no. 05P15RFCA1. H.N. has received funding from the European Union's Horizon 2020 research and innovation programme under the Marie Skłodowska-Curie grant agreement no. 655285. E.M. and H.N. were partially supported by the Helmholtz International Center for FAIR within the framework of the LOEWE program launched by the State of Hesse.

Appendix A: Thermodynamic integrals in the massless Boltzmann limit

Here we evaluate the thermodynamic integrals assuming Boltzmann statistics in the massless limit. In the LR

frame, where $u_{LR}^\mu = (1, 0, 0, 0)$, Eq. (4) reads

$$f_{0\mathbf{k}} \equiv \exp(\alpha_0 - \beta_0 E_{\mathbf{k}u}) = \lambda_0 \exp\left(-\beta_0 \sqrt{m_0^2 + k^2}\right), \quad (\text{A1})$$

where the fugacity is $\lambda_0 = \exp \alpha_0$ and $E_{\mathbf{k}u, LR} = k_0$. Similarly, the RS distribution function (30) reads in the LR frame

$$\begin{aligned} \hat{f}_{RS} &\equiv \exp\left(\alpha_{RS} - \beta_{RS} \sqrt{E_{\mathbf{k}u}^2 + \xi E_{\mathbf{k}l}^2}\right) \\ &= \lambda_{RS} \exp\left(-\beta_{RS} \sqrt{m_0^2 + k^2 + \xi k_z^2}\right), \end{aligned} \quad (\text{A2})$$

where the fugacity is $\lambda_{RS} = \exp \alpha_{RS}$ and $E_{\mathbf{k}l, LR} = k_z$.

Using these distribution functions the different thermodynamic integrals appearing in Eqs. (32) and (34) are evaluated in spherical coordinates, where $k = |\mathbf{k}|$, $k_x = k \cos \varphi \sin \theta$, $k_y = k \sin \varphi \sin \theta$, $k_z = k \cos \theta$. Therefore, $dK \equiv A_0 \frac{d^3 \mathbf{k}}{k_0^3} = A_0 \frac{k^2}{k_0^2} dk \sin \theta d\theta d\varphi$, where $\theta \in [0, \pi]$, $\varphi \in [0, 2\pi]$, $k \in [0, \infty)$, and $A_0 = g/(2\pi)^3$. Furthermore, we will also need the LR frame values of $-(\Delta^{\alpha\beta} k_\alpha k_\beta)_{LR} = k^2$ and $-(\Xi^{\mu\nu} k_\mu k_\nu)_{LR} \equiv k_\perp^2 = k_x^2 + k_y^2 = k^2 \sin^2 \theta$.

In the massless limit, i.e., $\lim_{m_0 \rightarrow 0} \sqrt{m_0^2 + k^2} = |k|$, we obtain the following result for Eq. (34),

$$\begin{aligned} \lim_{m_0 \rightarrow 0} I_{nq} &\equiv \lambda_0 \frac{(-1)^{2q} 4\pi A_0}{(2q+1)!!} \int_0^\infty dk k^{n+1} \exp(-\beta_0 k) \\ &= \lambda_0 \frac{4\pi A_0 (n+1)!}{\beta_0^{n+2} (2q+1)!!}. \end{aligned} \quad (\text{A3})$$

Here we list some of these integrals explicitly,

$$I_{00}(\alpha_0, \beta_0) \equiv I_{000} = \lambda_0 \frac{4\pi A_0}{\beta_0^2}, \quad (\text{A4})$$

$$I_{10}(\alpha_0, \beta_0) \equiv I_{100} = \lambda_0 \frac{8\pi A_0}{\beta_0^3} = n_0, \quad (\text{A5})$$

$$I_{20}(\alpha_0, \beta_0) \equiv I_{200} = \lambda_0 \frac{24\pi A_0}{\beta_0^4} = e_0, \quad (\text{A6})$$

$$I_{21}(\alpha_0, \beta_0) \equiv I_{201} = I_{220} = P_0, \quad (\text{A7})$$

where $P_0 \equiv n_0/\beta_0 = e_0/3$, and

$$I_{30}(\alpha_0, \beta_0) \equiv I_{300} = \lambda_0 \frac{96\pi A_0}{\beta_0^5}, \quad (\text{A8})$$

$$I_{31}(\alpha_0, \beta_0) \equiv I_{301} = I_{320} = \frac{I_{30}(\alpha_0, \beta_0)}{3}. \quad (\text{A9})$$

The RS distribution function leads to the following thermodynamical integral in the massless limit,

$$\begin{aligned} \lim_{m_0 \rightarrow 0} \hat{I}_{nrq}^{RS} &\equiv \lambda_{RS} \frac{(-1)^{2q} 2\pi A_0}{(2q)!!} \int_0^\pi d\theta \cos^r \theta \sin^{2q+1} \theta \\ &\times \int_0^\infty dk k^{n+1} \exp\left[-\beta_{RS} k \sqrt{1 + \xi \cos^2 \theta}\right] \\ &= \lambda_{RS} \frac{2\pi A_0 (n+1)!}{\beta_{RS}^{n+2} (2q)!!} \int_0^\pi d\theta \frac{\cos^r \theta \sin^{2q+1} \theta}{(1 + \xi \cos^2 \theta)^{\frac{n+2}{2}}}. \end{aligned} \quad (\text{A10})$$

Therefore, the ratio between the RS and equilibrium thermodynamical integrals defined in Eq. (33) reads

$$R_{nrq} = \frac{(2q+1)!!}{2(2q)!!} \int_0^\pi d\theta \frac{\cos^r \theta \sin^{2q+1} \theta}{(1 + \xi \cos^2 \theta)^{\frac{n+2}{2}}}, \quad (\text{A11})$$

hence the values that correspond to Eqs. (37) – (40) are

$$R_{100}(\xi) = \frac{1}{\sqrt{1+\xi}}, \quad (\text{A12})$$

$$R_{200}(\xi) = \frac{1}{2} \left(\frac{1}{1+\xi} + \frac{\arctan \sqrt{\xi}}{\sqrt{\xi}} \right), \quad (\text{A13})$$

$$R_{201}(\xi) = \frac{3}{2\xi} \left[\frac{1}{1+\xi} - (1-\xi) R_{200}(\xi) \right], \quad (\text{A14})$$

$$R_{220}(\xi) = -\frac{1}{\xi} \left[\frac{1}{1+\xi} - R_{200}(\xi) \right]. \quad (\text{A15})$$

Note that these results were obtained previously by Martinez and Strickland, see for example Ref. [18], such that $R_{100} = \mathcal{R}_0$ and $R_{200} = \mathcal{R}$, $R_{201} = \mathcal{R}_T$, while the last term differs from the results of Ref. [18] by a factor of $I_{20}/I_{21} = 3$ since they calculated $\hat{I}_{220}^{RS}/I_{21} = 3R_{220}(\xi)$, i.e., $R_{220} = \mathcal{R}_L/3$.

Furthermore, for the other moment equations (58), (62), (63), (64), (65), and (66) we also need the following $R_{nrq}(\xi)$ ratios

$$R_{000}(\xi) = \frac{\arctan \sqrt{\xi}}{\sqrt{\xi}}, \quad R_{020}(\xi) = \frac{1 - R_{000}(\xi)}{\xi}, \quad (\text{A16})$$

$$R_{240}(\xi) = \frac{1}{\xi^2} \left[\frac{3+\xi}{1+\xi} - 3R_{200}(\xi) \right], \quad (\text{A17})$$

$$R_{300}(\xi) = \frac{3+2\xi}{3(1+\xi)^{3/2}}, \quad R_{301}(\xi) = R_{100}(\xi), \quad (\text{A18})$$

$$R_{320}(\xi) = \frac{1}{3(1+\xi)^{3/2}}, \quad (\text{A19})$$

$$R_{440}(\xi) = -\frac{1}{8\xi^2} \left(\frac{3+5\xi}{(1+\xi)^2} - 3 \frac{\arctan \sqrt{\xi}}{\sqrt{\xi}} \right), \quad (\text{A20})$$

$$R_{460}(\xi) = \frac{1}{8\xi^3} \left(\frac{15+25\xi+8\xi^2}{(1+\xi)^2} - 15 \frac{\arctan \sqrt{\xi}}{\sqrt{\xi}} \right), \quad (\text{A21})$$

$$R_{540}(\xi) = \frac{1}{5(1+\xi)^{5/2}}. \quad (\text{A22})$$

Note that, for any odd r , $\hat{I}_{nrq}^{RS} = 0$.

Appendix B: Second-order fluid dynamics in the limit of small anisotropy

Here we recall the equations of second-order fluid dynamics describing the 0+1 dimensional boost-invariant expansion. Neglecting bulk viscosity we have

$$\frac{\partial e_0}{\partial \tau} = -\frac{1}{\tau} (e_0 + P_0 - \pi), \quad (\text{B1})$$

$$\tau_\pi \frac{\partial \pi}{\partial \tau} = \frac{4}{3} \frac{\eta}{\tau} - \pi - \left(\frac{1}{3} \tau_{\pi\pi} + \delta_{\pi\pi} \right) \frac{\pi}{\tau}, \quad (\text{B2})$$

where the equation for particle-number conservation is given in Eq. (56). Here $\pi = \pi^{00} - \pi^{zz}$ enters the shear-stress tensor $\pi^{\mu\nu} \equiv T^{\alpha\beta} \Delta_{\alpha\beta}^{\mu\nu} = \text{diag}(0, \pi/2, \pi/2, -\pi)$, where the corresponding symmetric, orthogonal, and traceless projection operator is $\Delta_{\alpha\beta}^{\mu\nu} = \frac{1}{2} (\Delta_{\alpha}^{\mu} \Delta_{\beta}^{\nu} + \Delta_{\beta}^{\mu} \Delta_{\alpha}^{\nu}) - \frac{1}{3} \Delta^{\mu\nu} \Delta_{\alpha\beta}$. Furthermore, the coefficients in the massless limit are, see for example Refs. [20, 45–48, 52],

$$\tau_{\pi\pi} = \frac{10}{7} \tau_{\pi}, \quad \delta_{\pi\pi} = \frac{4}{3} \tau_{\pi}. \quad (\text{B3})$$

These equations and coefficients can be derived by using the method of moments [48], where $\pi^{\mu\nu} = \int dK k^{\langle\mu} k^{\nu\rangle} \delta f_{\mathbf{k}}$ and $\delta f_{\mathbf{k}} = f_{\mathbf{k}} - f_{0\mathbf{k}}$ is the deviation from the equilibrium distribution function.

In the present case a similar approximation leads to $\hat{f}_{\mathbf{k}} = f_{0\mathbf{k}} + \delta f_{\mathbf{k}}(\xi)$ which corresponds to a series expansion of the fluid-dynamical quantities for small ξ . Expanding Eqs. (59) and (60) and neglecting corrections of order $\mathcal{O}(\xi^2)$ we obtain

$$\hat{P}_l \equiv e_0 \left(\frac{1}{3} - \frac{8}{45} \xi \right) = P_0 - \pi, \quad (\text{B4})$$

$$\hat{I}_{240}^{RS} \equiv e_0 \left(\frac{1}{5} - \frac{16}{105} \xi \right) = \frac{3}{5} P_0 - \frac{6}{7} \pi. \quad (\text{B5})$$

Applying these results to Eqs. (57) and (58) together with Eq. (55) we get

$$\tau_{eq} \frac{\partial \pi}{\partial \tau} = \frac{4}{3} \frac{\eta}{\tau} - \pi - \frac{38}{21} \frac{\pi}{\tau} \tau_{eq}. \quad (\text{B6})$$

which, after noting that in RTA $\tau_{eq} = \tau_{\pi}$, leads precisely to Eq. (B2). In the massive case it was shown [49] that this closure leads to the fluid-dynamical limit calculated in Refs. [45, 46], which in the massless case reduces to Eq. (B6).

Appendix C: Numerical solution of the Boltzmann equation in the RTA

For the sake of completeness we will repeat the discussion related to the numerical solution of the Boltzmann equation based on the derivation of Refs. [43, 44]. Let us first introduce the following Lorentz-invariant variables,

$$v \equiv \tau E_{\mathbf{k}u} = k_0 t - k_z z = \sqrt{w^2 + (k_{\perp}^2 + m_0^2) \tau^2}, \quad (\text{C1})$$

$$w \equiv \tau E_{\mathbf{k}l} = k_z t - k_0 z = \sqrt{v^2 - (k_{\perp}^2 + m_0^2) \tau^2}. \quad (\text{C2})$$

The inverse transformation reads

$$k_0 \equiv \frac{vt + wz}{\tau^2} = \frac{\cosh \eta}{\tau} (v + w \tanh \eta), \quad (\text{C3})$$

$$k_z \equiv \frac{wt + vz}{\tau^2} = \frac{\cosh \eta}{\tau} (w + v \tanh \eta). \quad (\text{C4})$$

Using these new boost-invariant variables the Boltzmann equation in RTA becomes a first-order linear differential equation

$$\frac{\partial f_{\mathbf{k}}}{\partial \tau} = \frac{f_{\mathbf{k}0} - f_{\mathbf{k}}}{\tau_{eq}}, \quad (\text{C5})$$

with the formal solution

$$f_{\mathbf{k}}(\tau) = D(\tau, \tau_0) f_{\mathbf{k}}(\tau_0) + \int_{\tau_0}^{\tau} \frac{d\tau'}{\tau_{eq}(\tau')} D(\tau, \tau') f_{\mathbf{k}0}(\tau'), \quad (\text{C6})$$

where $D(\tau_2, \tau_1)$ is a so-called damping function

$$D(\tau_2, \tau_1) = \exp \left(- \int_{\tau_1}^{\tau_2} \frac{d\tau'}{\tau_{eq}(\tau')} \right). \quad (\text{C7})$$

In order to obtain the relevant quantities we will need to calculate the moments of the solution (C6). Hence, similarly to Eq. (6), we calculate the moments of the equilibrium and anisotropic distribution functions. The equilibrium thermodynamic integrals $I_{nrq}(\tau, \tau', \alpha_0(\tau'), \beta_0(\tau')) = I_{nrq}$ read

$$\begin{aligned} I_{nrq} &\equiv \frac{(-1)^q}{(2q)!!} \int dK E_{\mathbf{k}u}^{n-r-2q} E_{\mathbf{k}l}^r (\Xi^{\mu\nu} k_{\mu} k_{\nu})^q f_{\mathbf{k}0}(\tau') \\ &= \frac{2\pi A_0 (n+1)!}{(2q)!!} \frac{\lambda_0(\tau')}{\beta_0^{n+2}(\tau')} H_{nrq}(\tau, \tau'), \end{aligned} \quad (\text{C8})$$

where we introduced the following integral:

$$H_{nrq}(\tau, \tau') = \int_0^{\pi} d\theta \frac{\cos^r \theta \sin^{2q+1} \theta}{\left[\left(\frac{\tau}{\tau'} \right)^2 \cos^2 \theta + \sin^2 \theta \right]^{\frac{n+2}{2}}}. \quad (\text{C9})$$

In some cases of interest these integrals were already calculated in Ref. [44], hence $H_{200}(\tau, \tau') = \mathcal{H}(\tau'/\tau)$, $H_{220}(\tau, \tau') = \mathcal{H}_L(\tau'/\tau)$ and $H_{201}(\tau, \tau') = \mathcal{H}_T(\tau'/\tau)$, see Eq. (A1) of Ref. [44]. Also note that these integrals were calculated using boost-invariant variables and additionally applying a second variable change, $p \cos \theta = \beta(\tau') w/\tau'$ and $p \sin \theta = \beta(\tau') k_{\perp}$.

Similarly, for the RS distribution function we have $\hat{I}_{nrq}^{RS}(\tau, \tau', \alpha_{RS}(\tau'), \beta_{RS}(\tau'), \xi(\tau')) = \hat{I}_{nrq}^{RS}$,

$$\begin{aligned} \hat{I}_{nrq}^{RS} &\equiv \frac{(-1)^q}{(2q)!!} \int dK E_{\mathbf{k}u}^{n-r-2q} E_{\mathbf{k}l}^r (\Xi^{\mu\nu} k_{\mu} k_{\nu})^q f_{RS}(\tau') \\ &= \frac{2\pi A_0 (n+1)!}{(2q)!!} \frac{\lambda_{RS}(\tau')}{\beta_{RS}^{n+2}(\tau')} H_{nrq} \left(\tau, \frac{\tau'}{\sqrt{1 + \xi(\tau')}} \right), \end{aligned} \quad (\text{C10})$$

where the argument of the H_{nrq} integral is scaled by a factor of $1/\sqrt{1 + \xi(\tau')}$ compared to Eq. (C8).

Now, applying the definition of the moments on both sides of Eq. (C6) together with the formal integral from Eq. (67),

$$F_{nrq}(\tau, \tau') = \frac{(-1)^q}{(2q)!!} \int dK E_{\mathbf{k}u}^{n-r-2q} E_{\mathbf{k}l}^r (\Xi^{\mu\nu} k_{\mu} k_{\nu})^q f_{\mathbf{k}}(\tau'), \quad (\text{C11})$$

we obtain an integral equation that can be solved for various initial conditions

$$F_{nrq}(\tau, \tau) = D(\tau, \tau_0)F_{nrq}(\tau, \tau_0) + \int_{\tau_0}^{\tau} \frac{d\tau'}{\tau_{eq}(\tau')} D(\tau, \tau') I_{nrq}(\tau, \tau') . \quad (\text{C12})$$

Assuming that the initial distribution function is of the RS form, i.e., $f_{\mathbf{k}}(\tau_0, k) = f_{RS}(\tau_0, k)$, leads to the following equation for the energy density, $e(\tau) = F_{200}(\tau, \tau)$,

$$e(\tau) = D(\tau, \tau_0) \hat{I}_{200}(\tau, \tau_0) + \int_{\tau_0}^{\tau} \frac{d\tau'}{\tau_{eq}(\tau')} D(\tau, \tau') I_{200}(\tau, \tau') . \quad (\text{C13})$$

However, since \hat{I}_{nrq} depends on a different set of parameters than I_{nrq} we also need to obtain $\alpha_{RS}(\tau)$ and $\beta_{RS}(\tau)$ in terms of the equilibrium quantities $\alpha_0(\tau)$ and $\beta_0(\tau)$ at $\tau = \tau_0$. This is done via the Landau matching conditions as shown in Sec. III, hence in case that particle number is not conserved, i.e., $\hat{I}_{200}(\tau_0, \tau_0) = I_{200}(\tau_0, \tau_0)$, Eqs. (C8) and (C10) lead to

$$\beta_{RS}(\tau_0) = \beta_0(\tau_0) \left[\frac{H_{200}(\tau_0, \tau_0/\sqrt{1+\xi_0})}{H_{200}(\tau_0, \tau_0)} \right]^{1/4}, \quad (\text{C14})$$

where $\xi_0 = \xi(\tau_0)$ while $H_{200}(\tau_0, \tau_0) = 2$ and so this expression is obviously equivalent to Eq. (48).

Finally, using the Landau matching condition for the l.h.s. of the integral equation $e(\tau) \equiv F_{200}(\tau, \tau) = I_{200}(\tau, \tau)$, we obtain the following equation for the evolution of the temperature

$$T^4(\tau) = T^4(\tau_0) D(\tau, \tau_0) \frac{H_{200}(\tau, \tau_0/\sqrt{1+\xi_0})}{H_{200}(\tau_0, \tau_0/\sqrt{1+\xi_0})} + \int_{\tau_0}^{\tau} \frac{d\tau'}{\tau_{eq}(\tau')} T^4(\tau') D(\tau, \tau') \frac{H_{200}(\tau, \tau')}{H_{200}(\tau, \tau)} . \quad (\text{C15})$$

In order to obtain the temperature as a function of proper time we use a combination of iteration and interpolation technique designed to obtain numerical solutions of integral equations [53].

Once the temperature is obtained we can calculate any moment of the distribution function from Eq. (C12) as

$$F_{nrq}(\tau) = \frac{2\pi A_0 (n+1)!}{(2q)!} \times \left[\frac{T^{n+2}(\tau_0) D(\tau, \tau_0)}{H_{200}^{-(n+2)/4}(\tau_0, \tau_0)} \frac{H_{nrq}(\tau, \tau_0/\sqrt{1+\xi_0})}{H_{200}^{(n+2)/4}(\tau_0, \tau_0/\sqrt{1+\xi_0})} + \int_{\tau_0}^{\tau} \frac{d\tau'}{\tau_{eq}(\tau')} T^{n+2}(\tau') D(\tau, \tau') H_{nrq}(\tau, \tau') \right] . \quad (\text{C16})$$

The method presented here can be extended to the case where particle number is conserved.

-
- [1] L.P. Csernai, *Introduction to Relativistic Heavy Ion Collisions*, (Wiley, Chichester, 1994).
- [2] L. Rezzolla and O. Zanotti, *Relativistic Hydrodynamics*, Second Edition, (Oxford University Press, Oxford, 2013).
- [3] T. Schaefer, *Ann. Rev. Nucl. Part. Sci.* **64**, 125 (2014) doi:10.1146/annurev-nucl-102313-025439 [arXiv:1403.0653 [hep-ph]].
- [4] P. Braun-Munzinger, V. Koch, T. Schfer and J. Stachel, *Phys. Rept.* **621**, 76 (2016) doi:10.1016/j.physrep.2015.12.003 [arXiv:1510.00442 [nucl-th]].
- [5] H. Niemi, G. S. Denicol, P. Huovinen, E. Molnar and D. H. Rischke, *Phys. Rev. Lett.* **106**, 212302 (2011) doi:10.1103/PhysRevLett.106.212302 [arXiv:1101.2442 [nucl-th]].
- [6] U. W. Heinz and R. Snellings, *Annu. Rev. Nucl. Part. Sci.* **63**, 123 (2013) [arXiv:1301.2826 [nucl-th]].
- [7] C. Gale, S. Jeon and B. Schenke, *Int. J. Mod. Phys. A* **28**, 1340011 (2013) [arXiv:1301.5893 [nucl-th]].
- [8] P. Huovinen, *Int. J. Mod. Phys. E* **22**, 1330029 (2013) [arXiv:1311.1849 [nucl-th]].
- [9] S. Ryu, J.-F. Paquet, C. Shen, G. S. Denicol, B. Schenke, S. Jeon and C. Gale, *Phys. Rev. Lett.* **115**, no. 13, 132301 (2015) doi:10.1103/PhysRevLett.115.132301 [arXiv:1502.01675 [nucl-th]].
- [10] H. Niemi, K. J. Eskola and R. Paatelainen, *Phys. Rev. C* **93**, no. 2, 024907 (2016) doi:10.1103/PhysRevC.93.024907 [arXiv:1505.02677 [hep-ph]].
- [11] H.W. Barz, B. Kampfer, B. Lukacs, K. Martinas and G. Wolf, *Phys. Lett. B* **194**, 15 (1987); B. Kampfer, B. Lukacs, G. Wolf and H.W. Barz, *Phys. Lett. B* **240**, 297 (1990); B. Kampfer, B. Lukacs, K. Martinas and H.W. Barz, KFKI-1990-47-A; B. Lukacs and A. Ster, arXiv:1112.5646 [hep-ph].
- [12] W. Florkowski, *Phys. Lett. B* **668**, 32 (2008) doi:10.1016/j.physletb.2008.07.101 [arXiv:0806.2268 [nucl-th]].
- [13] W. Florkowski and R. Ryblewski, *Phys. Rev. C* **83**, 034907 (2011) [arXiv:1007.0130 [nucl-th]].
- [14] R. Ryblewski and W. Florkowski, *J. Phys. G* **38**, 015104 (2011) [arXiv:1007.4662 [nucl-th]].
- [15] R. Ryblewski and W. Florkowski, *Eur. Phys. J. C* **71**, 1761 (2011) [arXiv:1103.1260 [nucl-th]].
- [16] R. Ryblewski and W. Florkowski, *Phys. Rev. C* **85**, 064901 (2012) [arXiv:1204.2624 [nucl-th]].
- [17] M. Martinez and M. Strickland, *Phys. Rev. C* **81**, 024906 (2010) [arXiv:0909.0264 [hep-ph]].
- [18] M. Martinez and M. Strickland, *Nucl. Phys. A* **848**, 183 (2010) [arXiv:1007.0889 [nucl-th]].
- [19] M. Martinez and M. Strickland, *Nucl. Phys. A* **856**, 68 (2011) [arXiv:1011.3056 [nucl-th]].
- [20] G. S. Denicol, W. Florkowski, R. Ryblewski and M. Strickland, *Phys. Rev. C* **90**, no. 4, 044905 (2014) doi:10.1103/PhysRevC.90.044905 [arXiv:1407.4767 [hep-ph]].

- [21] D. Bazow, U.W. Heinz and M. Strickland, *Phys. Rev. C* **90**, no. 5, 054910 (2014) [arXiv:1311.6720 [nucl-th]].
- [22] D. Bazow, M. Martinez and U. W. Heinz, *Phys. Rev. D* **93**, 034002 (2016) arXiv:1507.06595 [nucl-th].
- [23] M. Nopoush, M. Strickland, R. Ryblewski, D. Bazow, U. Heinz and M. Martinez, *Phys. Rev. C* **92**, no. 4, 044912 (2015) doi:10.1103/PhysRevC.92.044912 [arXiv:1506.05278 [nucl-th]].
- [24] P. Romatschke and M. Strickland, *Phys. Rev. D* **68**, 036004 (2003) [hep-ph/0304092].
- [25] M. Nopoush, R. Ryblewski and M. Strickland, *Phys. Rev. C* **90**, no. 1, 014908 (2014) doi:10.1103/PhysRevC.90.014908 [arXiv:1405.1355 [hep-ph]].
- [26] M. Alqahtani, M. Nopoush and M. Strickland, *Phys. Rev. C* **92**, no. 5, 054910 (2015) doi:10.1103/PhysRevC.92.054910 [arXiv:1509.02913 [hep-ph]].
- [27] W. Florkowski, E. Maksymiuk, R. Ryblewski and L. Tinti, *Phys. Rev. C* **92**, no. 5, 054912 (2015) doi:10.1103/PhysRevC.92.054912 [arXiv:1508.04534 [nucl-th]].
- [28] L. Tinti and W. Florkowski, *Phys. Rev. C* **89**, no. 3, 034907 (2014) [arXiv:1312.6614 [nucl-th]]; W. Florkowski, R. Ryblewski, M. Strickland and L. Tinti, *ibid.*, 054909 (2014) [arXiv:1403.1223 [hep-ph]]; L. Tinti, *Phys. Rev. C* **92**, no. 1, 014908 (2015) [arXiv:1411.7268[nucl-th]].
- [29] E. Molnar, H. Niemi and D. H. Rischke, *Phys. Rev. D* **93**, 114025 (2016) doi:10.1103/PhysRevD.93.114025 arXiv:1602.00573 [nucl-th].
- [30] J.D. Bjorken, *Phys. Rev. D* **27**, 140 (1983).
- [31] P.L. Bhatnagar, E.P. Gross and M. Krook, *Phys. Rev.* **94**, 511 (1954).
- [32] J.L. Anderson and H. R. Witting, *Physica* **74**, 466 (1974).
- [33] M. Gedalin, *Phys. Fluids B* **3**, 1871 (1991).
- [34] M. Gedalin and I. Oiberman, *Phys. Rev. E* **51**, 4901 (1995).
- [35] X.-G. Huang, M. Huang, D.H. Rischke and A. Sedrakian, *Phys. Rev. D* **81**, 045015 (2010) [arXiv:0910.3633 [astro-ph.HE]].
- [36] X.-G. Huang, A. Sedrakian and D.H. Rischke, *Annals Phys.* **326**, 3075 (2011) [arXiv:1108.0602 [astro-ph.HE]].
- [37] S.R. de Groot, W.A. van Leeuwen and Ch.G. van Weert, *Relativistic Kinetic Theory - Principles and applications*, (North Holland, Amsterdam, 1980).
- [38] C. Cercignani and G.M. Kremer, *The Relativistic Boltzmann Equation: Theory and Applications*, (Birkhäuser, Basel, 2002).
- [39] F. Jüttner, *Ann. Phys.* **339**, 856 (1911).
- [40] F. Jüttner, *Z. Phys.* **47**, 542 (1928).
- [41] C. Eckart, *Phys. Rev.* **58**, 919 (1940).
- [42] L.D. Landau and E.M. Lifshitz, *Fluid Dynamics*, Second Edition, (Butterworth-Heinemann, Oxford, 1987).
- [43] W. Florkowski, R. Ryblewski and M. Strickland, *Nucl. Phys. A* **916**, 249 (2013) doi:10.1016/j.nuclphysa.2013.08.004 [arXiv:1304.0665 [nucl-th]].
- [44] W. Florkowski, R. Ryblewski and M. Strickland, *Phys. Rev. C* **88**, 024903 (2013) doi:10.1103/PhysRevC.88.024903 [arXiv:1305.7234 [nucl-th]].
- [45] A. Jaiswal, *Phys. Rev. C* **87**, no. 5, 051901 (2013) doi:10.1103/PhysRevC.87.051901 [arXiv:1302.6311 [nucl-th]].
- [46] A. Jaiswal, R. Ryblewski and M. Strickland, *Phys. Rev. C* **90**, no. 4, 044908 (2014) doi:10.1103/PhysRevC.90.044908 [arXiv:1407.7231 [hep-ph]].
- [47] G.S. Denicol, E. Molnár, H. Niemi and D.H. Rischke, *Eur. Phys. J. A* **48**, 170 (2012) [arXiv:1206.1554 [nucl-th]].
- [48] G.S. Denicol, H. Niemi, E. Molnar and D.H. Rischke, *Phys. Rev. D* **85**, 114047 (2012) [Erratum-*ibid.* **D 91**, no. 3, 039902 (2015)] [arXiv:1202.4551 [nucl-th]].
- [49] L. Tinti, *Phys. Rev. C* **94**, no. 4, 044902 (2016) doi:10.1103/PhysRevC.94.044902 [arXiv:1506.07164 [hep-ph]].
- [50] G. S. Denicol, T. Koide and D. H. Rischke, *Phys. Rev. Lett.* **105**, 162501 (2010) doi:10.1103/PhysRevLett.105.162501 [arXiv:1004.5013 [nucl-th]].
- [51] W. Israel and J.M. Stewart, *Annals Phys.* **118**, 341 (1979).
- [52] G. S. Denicol, S. Jeon and C. Gale, *Phys. Rev. C* **90**, no. 2, 024912 (2014) doi:10.1103/PhysRevC.90.024912 [arXiv:1403.0962 [nucl-th]].
- [53] S. Richardson *The Mathematica Journal* **9** 2 (2014).